The challenges of containing SARS-CoV-2 via test-trace-and-isolate

Sebastian Contreras[1], **Jonas Dehning**[1], **Matthias Loidolt**[1], **F. Paul Spitzner**[1], **Jorge H. Urrea-Quintero**[1], **Sebastian B. Mohr**[1], **Michael Wilczek**[1,3], **Johannes Zierenberg**[1], **Michael Wibral**[2], **and Viola Priesemann**[1,3*]

[1]Max Planck Institute for Dynamics and Self-Organization, Am Faßberg 17, 37077 Göttingen, Germany.
[2]Campus Institute for Dynamics of Biological Networks, University of Göttingen, Hermann-Rein-Straße 3, 37075 Göttingen, Germany.
[3]Institute for the Dynamics of Complex Systems, University of Göttingen, Friedrich-Hund-Platz 1, 37077 Göttingen, Germany.

Abstract

Without a cure, vaccine, or proven long-term immunity against SARS-CoV-2, test-trace-and-isolate (TTI) strategies present a promising tool to contain the viral spread. For any TTI strategy, however, a major challenge arises from pre- and asymptomatic transmission as well as TTI-avoiders, which contribute to "hidden", unnoticed infection chains. In our semi-analytical model, we identified two distinct tipping points between controlled and uncontrolled spreading: one, at which the behavior-driven reproduction number R_t^H of the hidden infections becomes too large to be compensated by the available TTI capabilities, and one at which the number of new infections starts to exceed the tracing capacity, causing a self-accelerating spread. We investigated how these tipping points depend on realistic limitations like limited cooperativity, missing contacts, and imperfect isolation, finding that TTI is likely not sufficient to contain the natural spread of SARS-CoV-2. Therefore, complementary measures like reduced physical contacts and improved hygiene probably remain necessary.

***K*eywords** COVID-19 · SARS-CoV-2 · Contact tracing · Test-Trace-Isolate TTI

Introduction

After SARS-CoV-2 started spreading rapidly around the globe in early 2020, many countries have successfully curbed the initial exponential rise in case numbers ("first wave"). Most of the successful countries employed a mix of measures combining hygiene regulations and mandatory physical distancing to reduce the reproduction number and the number of new infections [1,2] together with testing, contact tracing, and isolation (TTI) of known cases [3,4]. Among these measures, those aimed at distancing — like school closures and a ban of all unnecessary social contacts ("strict lockdown") — were highly controversial, but have proven effective [1,2]. Notwithstanding, distancing measures put an enormous burden on society and economy. In countries that have controlled the initial outbreak, there is a strong motivation to relax distancing measures, albeit under the constraint to keep the spread of COVID-19 under control [5].

In principle, it seems possible that both goals can be reached when relying on the increased testing capacity for SARS-CoV-2 infections if complemented by contact tracing and quarantine measures (e.g. like TTI strategies [4]); South Korea and Singapore illustrate the success of such a strategy [6–8]. In practice, resources for testing are still limited and costly, and health systems have capacity limits for the number of contacts that can be traced and isolated; these resources have to be allocated wisely in order to control disease spread [9].

---

*viola.priesemann@ds.mpg.de
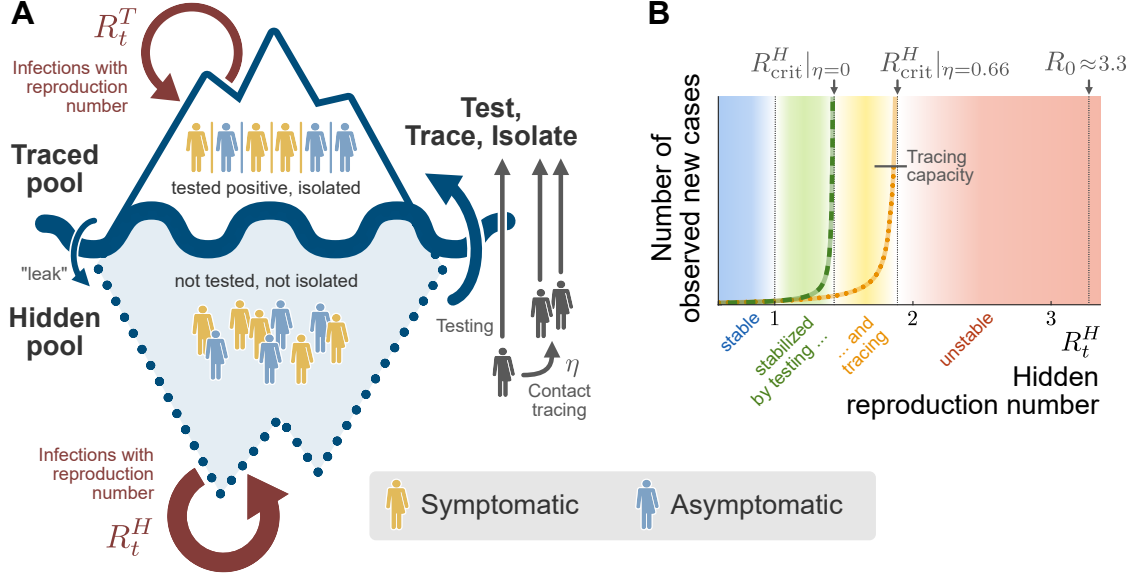
Figure 1: **Graphical abstract - summarizing the study**

TTI strategies have to overcome several challenges to be effective. Infected individuals can become infectious before developing symptoms [10,11], and because the virus is quite infectious, it is crucial to minimize testing and tracing delays [12]. Furthermore, SARS-CoV-2 infections surfacing widely distributed (instead of in clusters), which hinders an efficient and quick implementation of TTI strategies.

Hence, the effects of central challenges that impact and potentially limit the effectiveness of TTI need to be incorporated together into one model of COVID-19 control, namely (1) the existence of asymptomatic, yet infectious carriers [13, 14] — which are a challenge for symptom-driven but not for random testing strategies; (2) the existence of a certain fraction of the population that is opposed to taking a test, even if symptomatic [15]; (3) the capacity limits of contact tracing and additional imperfections due to imperfect memory or non-cooperation of the infected. Lastly, a certain influx of COVID-19 cases into a given community seems unavoidable at present due to the global spread of SARS-CoV-2, the relaxation of travel restrictions and the level of interconnection of some localities [5, 16]. This influx makes virus eradication impossible; it only leaves a stable level of new infections or their uncontrolled growth as the two possible regimes of disease dynamics. Thus, policy makers at all levels, from nations to federal states, all the way down to small units like enterprises, universities or schools, are faced with the question of how to relax physical distancing measures while confining COVID-19 progression with the available testing and contact-tracing capacity [17].

Here we employ a compartmental model of SARS-CoV-2 spreading dynamics that incorporates the challenges (1)-(3). We base the model parameters on literature or reports using the example of Germany. The aim is to determine the critical value for the reproduction number in the general (not quarantined) population (R_{crit}^H), for which disease spread can still be contained. We find that — even under an optimal use of the available testing and contract tracing capacity — the *hidden* reproduction number R_t^H has to be maintained at sufficiently low levels, namely $R_t^H < R_{\mathrm{crit}}^H \approx 2$ (95 % CI: 1.42–2.70). Hence, hygiene and physical distancing measures are required in addition to TTI to keep the virus spread under control.

To further assist the efficient use of resources, we investigate the relative merits of contact tracing, symptom-driven and random testing. We demonstrate the danger of a tipping point associated to the limited capacity of tracing contacts of infected people. Last but not least, we show how either testing scheme has to be increased to re-stabilize disease spread after an increase in the reproduction number.

Results

Model Overview

We developed an SIR-type model [18,19] with multiple compartments that incorporates the effects of test-trace-and-isolate (TTI) strategies (for a graphical representation of the model see Figs. 2,S1). We explore

how TTI can contain the spread of SARS-CoV-2 for realistic scenarios based on the TTI system in Germany. A major difficulty in controlling the spread of SARS-CoV-2 are the cases that remain hidden and behave as the general population does, potentially having many contacts. We explicitly incorporate such a "hidden" pool H into our model and characterize the spread within by the reproduction number R_t^H, which reflects the population's contact behavior. Cases remain hidden until they enter a "traced" pool through testing or by contact tracing of an individual that has already been tested positive (see Fig. 2). All individuals in the traced pool T isolate themselves (quarantine), reducing the reproduction number to R_t^T. Apart from a small leak, novel infections therein are then assumed to remain within the traced pool. We investigate both symptom-driven and random testing, which differ in the cases they can reveal: random testing can in principle uncover even asymptomatic cases, while symptom-driven testing is limited to symptomatic cases willing to be tested. Parameters describing the spreading dynamics (Tab. 1) are based on the available literature on COVID-19 [14, 15, 20–22], while parameters describing the TTI system are inspired by our example case Germany wherever possible.

We provide the code of the different analyses at `https://github.com/Priesemann-Group/covid19_tti`. An interactive platform to simulate scenarios different from those presented here is available (beta-version) on the same GitHub repository.
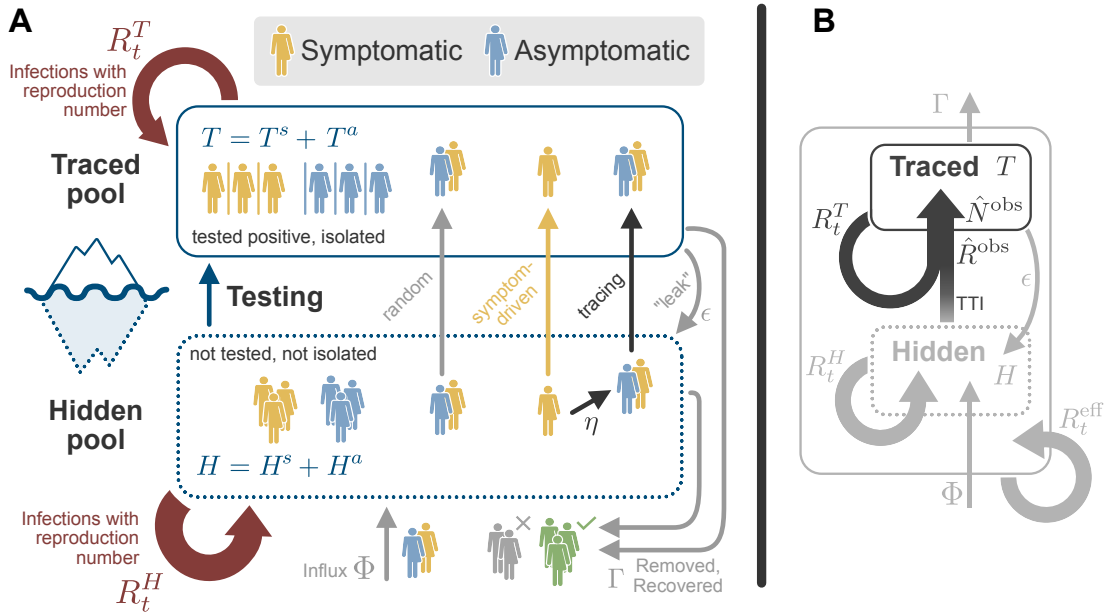
Figure 2: **Illustration of interactions between the hidden H and traced T pools in our model.** In our model, we distinguish two different infected population groups: the one that contains the infected individuals that remain undetected until tested (hidden pool H), and the one with infected individuals that we already follow and isolate (traced pool T). Until noticed, an outbreak will fully occur in the hidden pool, where case numbers increase according to this pool's reproduction number R_t^H. Testing and tracing of hidden infections transfers them to the traced pool and helps to empty the hidden pool; this prevents offspring infections and reduces the overall growth of the outbreak. Due to the self-isolation imposed in the traced pool, its reproduction number R_t^T is expected to be considerably smaller than R_t^H (i.e. $R_t^T \ll R_t^H$), and typically smaller than 1. Once an individual is tested positive, all the contacts since the infection are traced with some efficiency (η). Two external events further increase the number of infections in the hidden pool, namely, the new contagions occurring in the traced pool that leak to the hidden pool (ϵ) and an external influx of infections (Φ). In the absence of new infections, pool sizes are naturally reduced due to recovery (or removal), proportional to the recovery rate Γ.

TTI strategies can in principle control disease spread.

To demonstrate that TTI strategies can in principle control the disease spread, we simulated a new outbreak starting in the hidden pool (Fig. 3). We assume that the outbreak is unnoticed initially, and then evaluate the effects of two alternative testing and contact tracing strategies starting at day 0: Contact tracing is either efficient, i.e. 66% ($\eta = 0.66$) of the contacts of a positively tested person are traced and isolated without delay ("efficient tracing"), or contact tracing is assumed to be less efficient, identifying only 33%

of the contacts ("inefficient tracing"). In both regimes, the default parameters are used (Tab. 1), which include symptom-driven testing with rate $\lambda_s = 0.1$, and isolation of all tested positively, which reduces their reproduction number by a factor of $\nu = 0.1$.
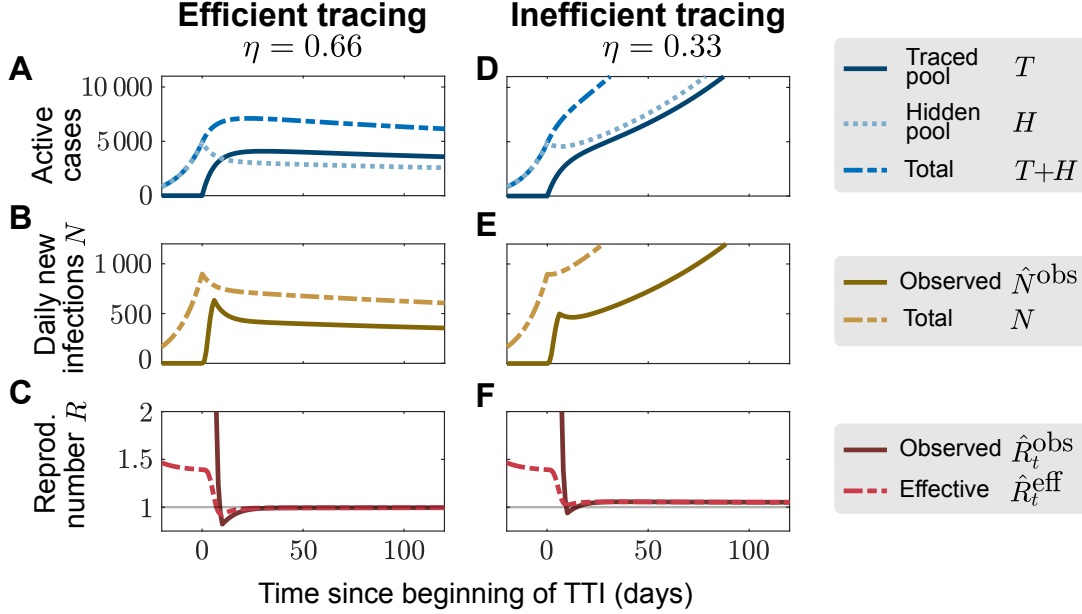

Figure 3: **Sufficient testing and contact tracing can control the disease spread, insufficient only slows it.** We consider a TTI strategy with symptom-driven testing ($\lambda_s = 0.1$) and two tracing scenarios: For high tracing efficiency ($\eta = 0.66$, **(A-C)**), the outbreak can be controlled by TTI; for low tracing efficiency ($\eta = 0.33$, **(D-E)**) the outbreak cannot be controlled because tracing is not efficient enough. **(A,D)** Number of infections in the hidden pool grows until the outbreak is noticed on day 0, at which point symptom-driven testing ($\lambda_s = 0.1$) and contact tracing (η) starts. **(B,E)** Absolute number of daily infections (N) grows until the outbreak is noticed on day 0; the observed number of daily infections ($\hat{N}^{\text{obs}}$) shown here is simulated as being inferred from the traced pool and subject to a gamma-distributed reporting delay with a median of 4 days. **(C,F)** The observed reproduction number $\hat{R}_t^{\text{obs}}$ is estimated from the observed new infections $\hat{N}^{\text{obs}}$. After an initial growth period, it settles to $\hat{R}_t^{\text{obs}} = 1$ if the outbreak is controlled (efficient tracing), or to $\hat{R}_t^{\text{obs}} > 1$ if the outbreak continues to spread (inefficient tracing).
All the curves plotted are obtained from numerical integration of equations (1) - (5).

Efficient contact tracing rapidly depletes the hidden pool H and populates the traced pool T, and thus stabilizes the total number of infections $T + H$ (Fig. 3A). The system relaxes to its equilibrium, which is a function of TTI and epidemiological parameters (equations (S2)–(S4) in section). Consequently, the observed number of daily infections ($\hat{N}^{\text{obs}}$) approaches a constant value (Fig. 3B), while the observed reproduction number $\hat{R}_t^{\text{obs}}$ approaches unity (Fig. 3C), further showing that effective TTI can be sufficient to stabilize the disease spread with $R_t^H = 1.8$.

In contrast, inefficient contact tracing cannot deplete the hidden pool sufficiently quickly to stabilize the total number of infections (Fig. 3D). Thus, the absolute and the observed daily number of infections N continue to grow approximately exponentially (Fig. 3E). In this case, the TTI strategy with ineffective contact tracing slows the spread, but cannot control the outbreak.

Test-trace-and-isolate strategies give rise to two novel stabilized regimes of spreading dynamics.

Comparing the two TTI strategies from above demonstrates that two distinct types of spreading dynamics are attainable under the condition of a non-zero influx of new cases Φ: The system either evolves towards some intermediate, but stable number of new cases N (Fig. 3A-C), or it is unstable, showing a steep growth (Fig. 3D-F). These two dynamics are characterized — after an initial transient — by different "observed" reproduction numbers $\hat{R}_t^{\text{obs}}$, inferred from the new cases of the traced pool $\hat{N}^{\text{obs}}$. If $\hat{R}_t^{\text{obs}} = 1$, the outbreak is under control (solid in Fig. 3C), while for $\hat{R}_t^{\text{obs}} > 1$ the outbreak continues to spread (Fig. 3F).

These two regimes (stable or growing) are known from the standard SIR model with external influx Φ (blue and red regions in Fig. 4A,B): If the reproduction number R is less than one, each new case infects less than one new case on average, and the number of new cases in equilibrium $\hat{N}_\infty^{obs}$ is finite (Fig. 4A). If R is above one, each new case infects more than one new case, and the number of new cases grows quickly. These regimes are reflected in the equilibrium observed reproduction number $\hat{R}_\infty^{obs}$: In the stable regime, $\hat{R}_\infty^{obs} = 1$, and in the unstable regime $\hat{R}_\infty^{obs} > 1$.
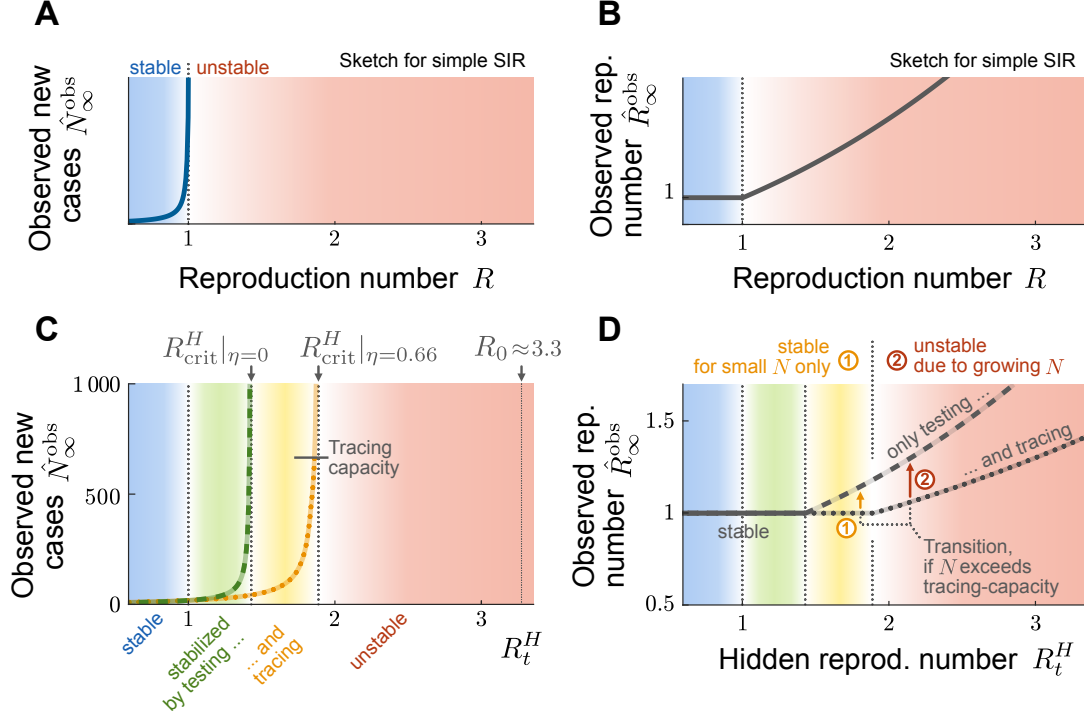
Figure 4: **Testing and tracing give rise to two novel stabilized regimes of spreading dynamics.** In the simple SIR model with external influx **(A,B)**, the spreading dynamics exhibit a stable and an unstable regime (blue and red regions, respectively). In addition to these, our two-pool model exhibits **(C,D)** two novel "stabilized" regimes that arise from the isolation of infected persons upon testing positive (green region) or upon being traced as a contact of an infected person (amber region). **(A)** Observed case numbers $\hat{N}_\infty^{obs}$ in the simple SIR model with external influx approach a finite equilibrium in the stable regime (blue solid line). As the reproduction number R approaches the critical point at $R = 1$, the case numbers in equilibrium $\hat{N}_\infty^{obs}$ diverge, growing uncontrolled in the unstable regime. **(B)** The asymptotic observed reproduction number $\hat{R}_\infty^{obs}$ inferred from the observed new cases $\hat{N}_\infty^{obs}$ in the simple SIR model with external influx is always 1 in the stable regime, but reflects the true value R in the unstable regime (solid grey line). **(C)** Daily number of new infections $\hat{N}_\infty^{obs}$ in our two-pool model are finite in the stable and stabilized regimes, but diverge upon approaching the critical points of the "testing only" or "testing and tracing" strategies (dashed green and dotted orange lines, respectively). They are infinite in the unstable regime, or when the tracing capacity limit is reached (black bar). The exact position of the critical points of the stabilized regimes depend on the efficiencies of the respective strategies: Symptom-driven testing alone ($\eta = 0$, green) can only stabilize the spread for $\hat{R}_\infty^{obs} < R_{\mathrm{crit}}^H|_{\eta=0} \approx 1.5$, while symptom-driven testing and tracing ($\eta = 0.66$, amber) can stabilize the spread for up to $R_t^H < R_{\mathrm{crit}}^H|_{\eta=0.66} \approx 1.9$ for our default parameters (Table. 1). **(D)** The observed reproduction number $\hat{R}_\infty^{obs}$ of a system stabilized by symptom-driven testing and tracing is always 1 in the "stable" and "testing-stabilized" regimes (solid grey line). In the meta-stable "testing-and-tracing-stabilized" regime (dotted grey line), $\hat{R}_\infty^{obs} = 1$ as long as the tracing capacity is not exceeded. If exceeded, the system behaves asymptotically as if there was only symptom-driven testing in place (transition "1", see also Fig. 5), which can only slow down, but not control the spread anymore. In the "unstable" regime, the observed reproduction number $\hat{R}_\infty^{obs}$ always increases with R_t^H – thus, the number of cases always grows. As long as the tracing capacity is not exceeded by this growth, testing-and-tracing slows down the spread (dotted grey line) – afterwards the system behaves asymptotically as if there was only symptom-driven testing slowing down the spread (transition "2", see also Fig. 6). The curves showing observed new cases are obtained from the analytical description of the equilibrium for unlimited tracing capacity (equations (S2) - (S4)). The curves showing the observed reproduction number are obtained from the linear stability analysis (equation (S1)).

Distinct from the standard SIR model, our two-pool model with TTI exhibits two novel stable regimes of spreading dynamics: The first regime requires only to isolate persons with positive test results ("testing-stabilized"), the second requires in addition to find and isolate contacts of a positively tested person ("tracing-stabilized", Fig. 4C,D). Due to the stabilization, the transition to instability for these two regimes is shifted towards hidden reproduction numbers R_t^H above one (dotted grey lines in Fig. 4C). As in the classical stable regime, the number of new cases in equilibrium $\hat{N}_\infty^{obs}$ diverges when approaching these novel critical points (dashed green and dotted orange lines in Fig. 4C). The ultimately unstable regime begins at $R_t^H = R_{crit}^H \simeq 1.9$ for our default parameters. Note that R_{crit}^H is below the basic reproduction number reported for SARS-CoV-2 ($R_0 \approx 3.3$), however, it may already be attained by reducing contacts by $40\,\%$ from levels at the beginning of the pandemic.

A limited tracing capacity renders the tracing-stabilized regime meta-stable.

The amount of contacts that can reliably be traced by health authorities is limited due to the work to be performed by trained personnel: Contact persons have to be identified, informed, and ideally also counseled during the preventive quarantine. Exceeding the tracing capacity limit destabilizes an otherwise stable regime, rendering it effectively meta-stable (amber in Fig. 4C,D). Once the tracing capacity is exceeded, the system will behave asymptotically as if it had testing only, i.e. the effective and observed reproduction number will strongly increase (transition "1") from dotted to dashed grey line in Fig. 4D).

This demonstrates that a low number of new infections is essential to control the spread when $R_t^H > 1$. Crossing the capacity limit of tracing, N_{max}, leads to a self-accelerating spread, and thereby presents a qualitatively new tipping point to instability in an otherwise stable system.

A limited tracing capacity requires a safety margin to avoid new outbreaks.

The transition from the meta-stable regime to the unstable regime happens when the tracing system is overwhelmed due to the number of observed new cases exceeding the tracing capacity ($\hat{N}^{obs} > N_{max}$). This can occur because of an increased influx Φ of infected people, e.g. returning from holiday, or a super-spreading event. As an example, we simulate here a short but large influx of 4000 cases within a few days at $t = 0$ (Fig. 5). We set two different capacity limits, reached at $N_{max} = 675$ (or $N_{max} = 450$) observed cases per day (see methods). In both scenarios, the sudden influx leads to a jump of infections in the hidden pool (Fig. 5A,D), followed by a fast increase in new traced cases (Fig. 5B,E). With sufficiently high tracing capacity, the outbreak can then be contained, because during the initial shock $\hat{N}^{obs}$ does not exceed the capacity limit N_{max} (Fig. 5B, brown vs grey lines). In contrast, with lower capacity, the outbreak accelerates as soon as the observed new cases $\hat{N}^{obs}$ exceeds the capacity limit N_{max}. In essence, this scenario demonstrates the meta-stability of the system introduced above; if the capacity limit is exceeded due to some external perturbation, the tracing cannot compensate the perturbation and the spread gets out of control.

An alternative transition can occur when a relaxation of contact restrictions causes a slow growth in case numbers. This slow growth accelerates dramatically after the tracing capacity limit is reached (Fig. 4D, transition "2" within the red region from dotted to dashed). Thus, this is a transition from a slightly unstable to a strongly unstable regime. To illustrate this, we simulated an increase of the hidden reproduction number R_t^H (of a system in stable equilibrium) at $t = 0$, from $R_t^H = 1.8$ to a supercritical value $R_t^H = 2$, which renders the system slightly unstable (Fig. 6). At $t = 0$, the case numbers start to grow slowly until the observed number of new cases exceeds the tracing capacity limit N_{max}. From thereon, the tracing system breaks down and the growth self-accelerates. This is reflected in the steep rise of new cases after day 100 - thus with a considerable delay after the change of R_t^H, i.e. the population's behavior.

Both the initial change in the hidden reproduction number and the breakdown of the tracing system are reflected in the observed reproduction number $\hat{R}_t^{obs}$ (Fig. 6C). It transits from stability ($\hat{R}_t^{obs} = 1$) to instability ($\hat{R}_t^{obs} > 1$). However, the absolute values of $\hat{R}_t^{obs}$ are not very indicative about the public's behavior (R_t^H), because already small changes in R_t^H can induce large transient changes in $\hat{R}_t^{obs}$. In our example, $\hat{R}_t^{obs}$ shows a strong deflection after $t = 0$, although R_t^H changes only slightly; later, at $t \approx 100$ it starts to ramp to a new value, although R_t^H did not change. This ramping is due to exceeding the tracing capacity N_{max}, and the spread starts to accelerate. $\hat{R}_t^{obs}$ finally approaches a new steady-state value, as sketched in Fig. 4D. To summarize, deducing the stability of the spread from $\hat{R}_t^{obs}$ is challenging because $\hat{R}_t^{obs}$ reacts very sensitively to many types of transients. R_t^H, in contrast, would be a reliable indicator of true spreading behavior, but is not accessible easily.
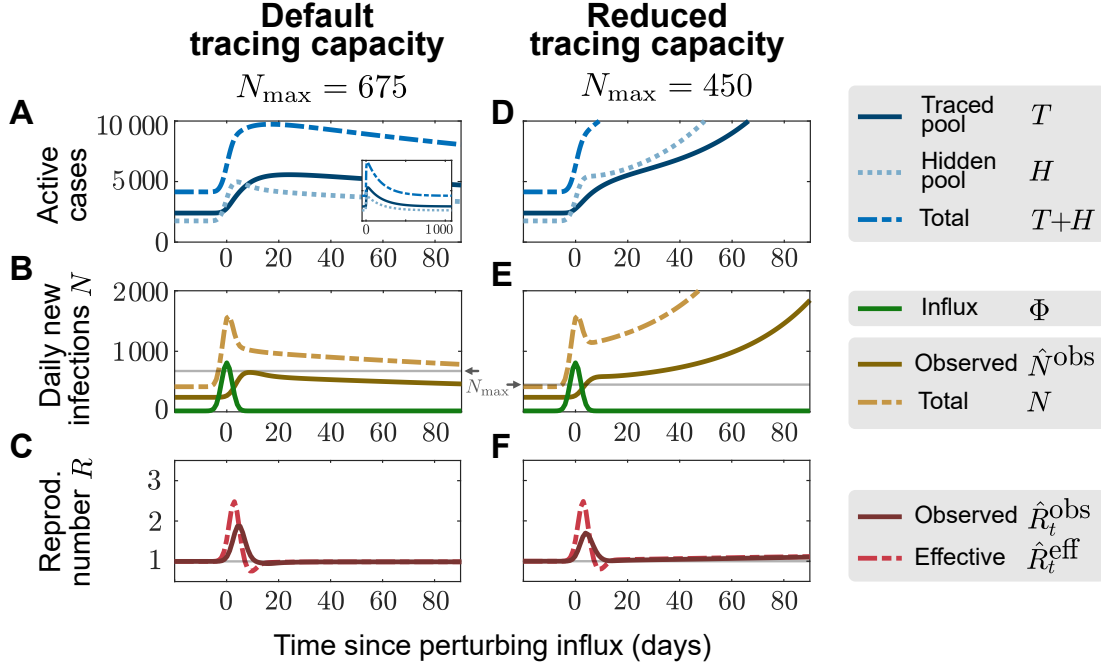
Figure 5: **Limited tracing capacity makes a meta-stable system vulnerable to large influx events.** A single large influx event (4000 cases) drives a meta-stable system with reduced tracing capacity (reached at $N_{\max} = 450$) to a new outbreak **(D-F)**, while a meta-stable system with our default tracing capacity (reached at $N_{\max} = 675$) can compensate a sudden influx of this size **(A-C)**. **(A,D)** Number of infections in the hidden pool (dotted) jump due to the influx event at t=0, and return to stability for default capacity (A) or continue to grow in the system with reduced capacity (D). Correspondingly, the number of cases in the traced pool (solid) either slowly increases after the event, and absorbs most infections before returning to stability (inset in A, time axis prolonged to 1000 days), or proceeds to grow steeply (D). **(B,E)** The absolute number of new infections (dashed, yellow) jumps due to the large influx event (solid, green). The daily observed cases (solid, brown) slowly increases after the event, and relaxes back to baseline (A), or increases fast upon exceeding the maximum number of new observed cases $N_{\max}$ (solid grey line) for which tracing is effective. **(C,F)** The effective (dashed, red) and observed (solid, dark red) reproduction numbers change transiently due to the influx event, before returning to one for the default tracing capacity. In the case of a reduced tracing capacity and a new outbreak, they slowly begin to grow afterwards (F). All the curves plotted are obtained from numerical integration of equations (1) - (5).

Containing the spread of SARS-CoV-2 probably requires both TTI strategies and contact-reduction policies.

Above, we illustrated that a combination of symptom-driven testing and contact tracing can control the outbreak for a default reproduction number of $R_t^H = 1.8$. We now ask how efficient the TTI scheme and implementation must be to control the disease for a range of reproduction numbers— i.e. what TTI parameters are necessary to avoid the tipping over to $\hat{R}_t^{\text{eff}} > 1$. When assessing stability not only for a single scenario along the R_t^H-axis, but for multiple parameter combinations, the tipping points turn into critical lines (or surfaces). Here, we examine how these critical lines depend on different combinations of symptom-driven testing, random testing, and contact tracing.

Random testing with tracing, but without symptom-driven testing ($\lambda_s = 0$), is not sufficient to contain an outbreak (under our default parameters and $R_t^H \leq 1.5$; Fig. 7A). This is because the rate of random testing λ_r would have to be unrealistically large. It exceeds the current capacity of testing ($\lambda_{r,\max} \sim 0.002$, see Methods for details), even if ten tests are pooled ($\lambda_r \sim 10\lambda_{r,\max}$ [23]). Thus, the contribution of symptom-driven testing is necessary to control any realistic new outbreak through TTI.

Contact tracing markedly contributes to outbreak mitigation (Fig. 7B). In its absence, i.e. when isolating only individuals that were positive in a symptom-driven or random test, the outbreak can be controlled for intermediate reproduction numbers ($R_t^H < 2.5$ in Fig. 7B) but not for higher ones if the limit of $\lambda_{r,\max} < 0.02$ is respected.
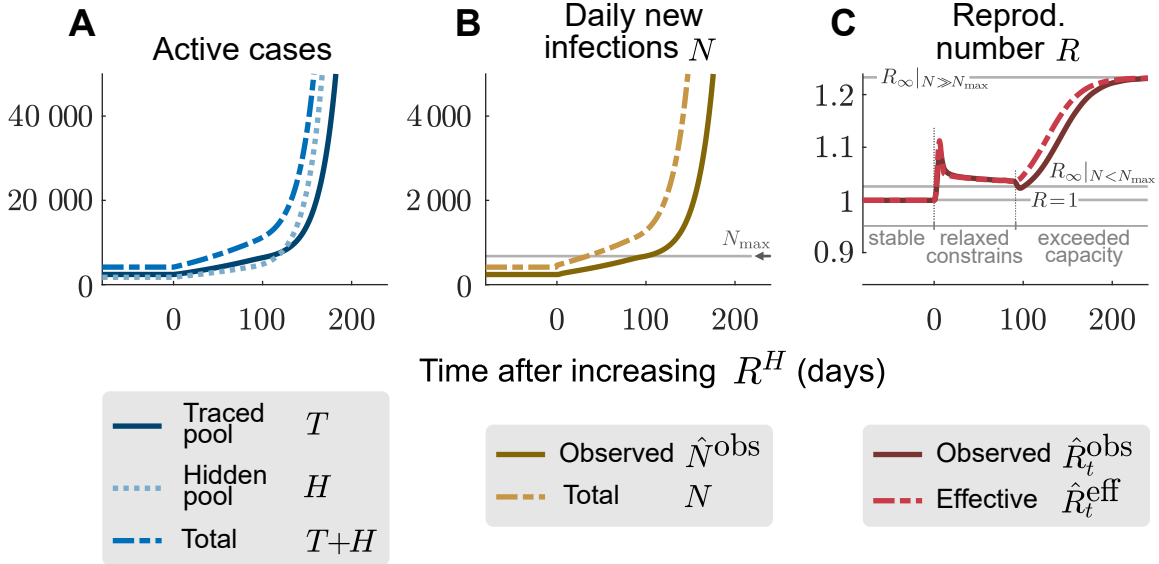
Figure 6: **Relaxing restrictions can slowly overwhelm the tracing capacity and trigger a new outbreak.** **(A)** The hidden reproduction number increases from $R_t^H = 1.8$ to $R_t^H = 2.0$ (i.e. slightly above its critical value) at $t = 0$ leads to a slow increase in traced active cases (solid blue). **(B)** When the number of observed new cases (solid brown) exceeds the tracing capacity limit $N_{\max}$ (solid grey), the tracing system breaks down and the outbreak starts to accelerate. **(C)** After an initial transient at the onset of the change in R_t^H, the observed reproduction number (solid red) faithfully reflects both the slight increase of the hidden reproduction number due to relaxation of contact constraints, and the strong increase after the tracing capacity (solid grey) is exceeded at $t \approx 100$. All the curves plotted are obtained from numerical integration of equations (1) - (5).

The most effective combination appears to be symptom-driven testing together with contact tracing (Fig. 7C). This combination shows stability even for spreads close to the basic reproduction number $R_t^H = R_0 \approx 3.3$, when implemented *extremely* efficiently (e.g. with $\lambda_s = 0.66$ and $\eta = 0.66$). However, this implementation would require that all symptomatic persons get tested within 1-2 days after getting infectious, thus potentially already in their pre-symptomatic phase, which may be difficult to realize. (Note that the asymptomatic cases are already accounted for in the model and do not pose an additional problem). Considering these difficulties, the combination of symptom-driven testing and contact tracing appears to be sufficient to contain outbreaks with *intermediate* reproduction numbers ($R_t^H \sim 2$ can be controlled with e.g. $\lambda_s \leq 0.5$ and $\eta = 0.66$, Fig. 7C).

Overall, our model suggests that the combination of timely symptom-driven testing within very few days, together with isolation of positive cases and efficient contact tracing can be sufficient to control the spread of SARS-CoV-2 given the reproduction number in the hidden pool is $R_t^H \approx 2$ or lower. For random testing to be effective, one would require much higher test rates than currently available in Germany.

Comparison of TTI strategies for compensating intermediate relaxation of contact constraints.

There are currently strong incentives to loosen restrictive measures and return more to a pre-COVID-19 lifestyle [24, 25]. Any such loosening, however, can lead to a higher reproduction number R_t^H, which could potentially exceed the critical value R_{crit}^H, for which current TTI strategies ensure stability. To retain stability despite increasing R_t^H, this increase has to be compensated by stronger mitigation efforts, such as further improvement of TTI. Thereby the critical value R_{crit}^H is effectively increased. In the following, we compare the capacity of the different TTI and model parameter changes to compensate for increases of the reproduction number R_t^H. In detail, we start from the highest reproduction number that can be controlled by the default parameters, $R_{\text{crit}}^H = 1.89$, and calculate how each model parameter would have to be changed to achieve a desired increase in R_{crit}^H. For all default parameters, see Table 1.

First, we explore how well an increase of random and symptom-driven test rates can compensate an increase in R_t^H (Fig. 8A). We find that random testing would need to increase extensively to compensate an increases in R_t^H, i.e. λ_r quickly exceeds realistic values (grey lines in Fig. 8A).
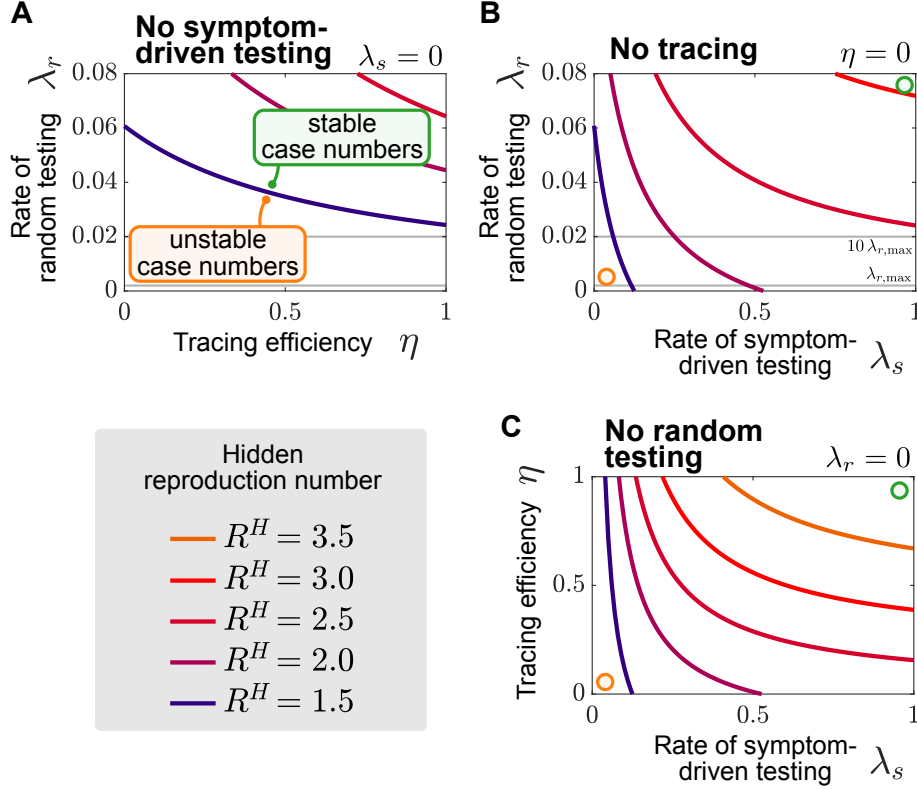
Figure 7: **Symptom-driven testing and contact tracing need to be combined to control the disease.** Stability diagrams showing the boundaries (continuous curves) between the stable (controlled) and uncontrolled regimes for different testing strategies combining random testing (rate λ_r), symptom-driven testing (rate λ_s), and tracing (efficiency η). grey lines in plots with λ_r-axes indicate capacity limits (for our example Germany) on random testing ($\lambda_{r,\max}$) and when using pooling of 10 samples, i.e. $10\lambda_{r,\max}$. Colored lines depict the transitions between the stable and the unstable regime for a given reproduction number R_t^H (colour-coded). The transition from *stable* to *unstable* case numbers is explicitly annotated for $R_t^H = 1.5$ in panel A. **(A)** Combining tracing and random testing without symptom-driven testing is in all cases not sufficient to control outbreaks, as the necessary random tests exceed even the pooled testing capacity ($10\lambda_{r,\max}$). **(B)** Combining random and symptom-driven testing strategies without any contract tracing requires unrealistically high levels of random testing to control outbreaks with large reproduction numbers in the hidden pool ($R_t^H > 2.0$). The required random tests to significantly change the stability boundaries exceed the available capacity in Germany $\lambda_{r,\max}$. Even taking into account the possibility of pooling tests ($10\lambda_{r,\max}$) often does not suffice to control outbreaks. **(C)** Combining symptom-driven testing and tracing suffices to control outbreaks with realistic testing rates λ_s and tracing efficiencies η for moderate values of reproduction numbers in the hidden pool, R_t^H, but fails to control the outbreak for large R_t^H. The curves showing the critical reproduction number are obtained from the linear stability analysis (equation (S1)).

In contrast, scaling up symptom-driven testing can in principle compensate an increase of R_t^H up to about 3 (Fig. 8A). Beyond $R_t^H = 3$ and $\lambda_s \approx 0.4$, λ_s increases more steeply, making this compensation increasingly costly (Fig. 8A). Furthermore, levels of $\lambda_s > 0.5$ seem hard to realize as they would require testing within < 2 days of becoming infectious, i.e. while many infected are still pre-symptomatic. Realistically, only moderate increases in R_t^H can be compensated by decreasing the average delay of symptom-driven testing alone.

Tracing the contacts of an infected person and asking them to quarantine preventively is an important contribution to contain the spread of SARS-CoV-2, if done without delay [3, 12]. As a default, we assumed that a fraction $\eta = 0.66$ of contacts are traced and isolated within a day. This fraction can in principle be increased further to compensate an increase in R_t^H and still guarantee stability (Fig. 8A). However, because η is already high in the first place, its range is quite limited, and even perfect contact tracing cannot compensate an R_t^H of 2.5.

As an alternative to improved TTI rates and efficiencies, improved compliance may compensate an increase in R_t^H: One might aim to reduce the number of contacts missed in the traced pool ϵ, improve the isolation factor

9
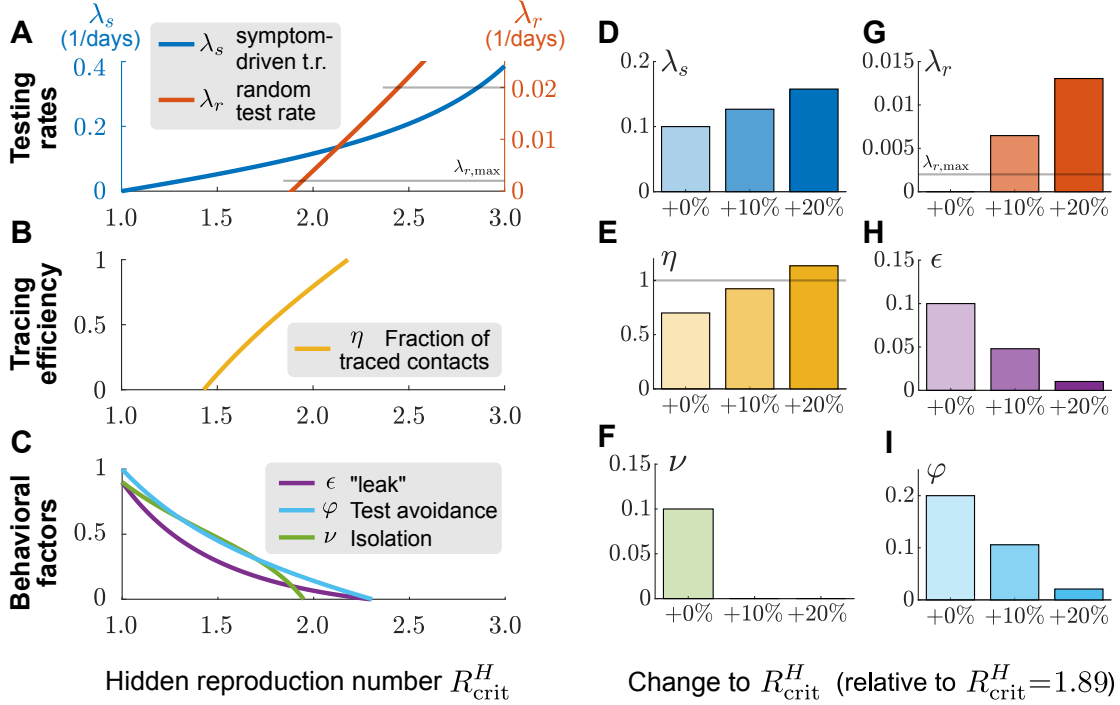
Figure 8: **Adapting testing strategies allows to relax contact constraints to some degree.** Relaxing contact constraints increases the reproduction number of the hidden pool R_t^H, and thus needs to be compensated for by adjusting model parameters in order to keep the system stable. **(A-C)** Value of a single parameter required to keep the system stable despite a change in the hidden reproduction number, while keeping all other parameters at default values. **(A)** Increasing the rate of symptom-driven testing λ_s (blue) can in principle compensate for hidden reproduction numbers close to R_0. This is optimistic, however, as it requires that anyone with symptoms compatible with COVID-19 gets tested and isolated on average within 2.5 days – requiring large resources and efficient organization. Increasing the random-testing rate λ_r (red) to the capacity limit (for the example Germany, grey line $\lambda_{r,\max}$) would have almost no effect, pooling tests to achieve $10\lambda_{r,\max}$ can compensate for somewhat for larger increases in R_t^H. **(B)** Increasing the tracing efficiency can compensate only small increases in R_t^H. **(C)** Decreasing the fraction of symptomatic individuals avoiding testing φ, the leak from the traced pool ϵ or the escape rate from isolation ν can in principle compensate for small increases in R_t^H. **(D-I)** To compensate a 10% or 20% increase of R_t^H, and still keep the system stable, symptom-driven testing λ_s could be increased (D), or ϵ or ϕ could be decreased (H,I). In contrast, only changing λ_r, η, or ν would not be sufficient to compensate a 10 % or 20 % increase in R_t^H, because their limits are reached (E,F,G). All parameter changes are computed through stability analysis (equation (S1)).

ν, or reduce the fraction of people avoiding tests despite showing symptoms φ (Fig. 8C). These improvements might be more difficult to achieve from a policy-maker perspective but could be targeted by educational and awareness-raising campaigns. However, since we assumed already in the default scenario that the behavioral factors (ϵ, ν, φ) are not too large, the potential improvement is limited.

The amount of reduction achievable by each method is limited, which calls to leverage all these strategies together. Furthermore, as can be seen from the curvature of the lines in Fig. 7, the beneficial effects are synergistic, i.e. they are larger when combining several strategies instead of spending twice the efforts on a unique one. This synergy of improved TTI measures and awareness campaigning could allow to relax contact constraints while keeping outbreaks under control. Nonetheless, our model still indicates that compensating the basic reproduction number $R_t^H = R_0 \approx 3.3$ might be very costly, and hence some degree of physical distancing might be required.

Robustness against parameter changes and model limitations

Above, we showed that changing the implementation of the TTI strategy can accommodate higher reproduction numbers R_{crit}^H – but how robust are these implementations against parameter uncertainties? To explore the robustness of the resulting hidden reproduction number R_{crit}^H against simultaneous variation of multiple TTI

parameters, we draw these parameters from beta distributions (because all parameters are bounded by 0 and 1) centered on the default values and perform an error propagation analysis (Table S1). We found that a hidden reproduction number of $R_t^H \leq 1.4$ (95 % CI, 1.23–1.69) can be compensated by testing alone, whereas additional contact tracing allows a hidden reproduction number of $R_t^H \leq 1.9$ (95 % CI, 1.42–2.70, Fig. S2, Tab. S1). This shows that the exact implementation of the TTI strategy strongly impacts the public behavior that can be controlled, but none of them allows for a complete lifting of contact restrictions ($R_0 = 3.3$).

Another aspect of robustness is not that against variation of parameters, but against variation of the model and the underlying assumptions. Our model also comes with some inevitable simplifications, but these do not compromise the conclusions drawn here. Specifically, our model is simple enough to allow for a mechanistic understanding of its dynamics and analytical treatment of the control and stability problems. Owing to its simplicity it has certain limitations: In contrast to agent-based simulations [26, 27], we do not include realistic contact structures [4, 5, 28] - the infection probability is uniform across the whole population. This limitation will become relevant mostly when trying to devise even more efficient testing and tracing strategies, and when a stabilization of a system very close to its tipping point is desired. Compared to other mean-field based studies which included a more realistic temporal evolution of infectiousness [29, 30], we implicitly assume that infectiousness decays exponentially. This assumption has the disadvantage of making the interpretation of rate parameters more difficult, but should not have an effect on the stability analyses presented here.

Discussion

Using a compartmental SIR-type model with realistic parameters based on our example case Germany, we find that test-trace-and-isolate can, in principle, contain the spread of SARS-CoV-2 if some physical distancing measures are continued. We analytically derived the existence of a novel meta-stable regime of spreading dynamics governed by the limited capacity of contact tracing and show how transient perturbations can tip a seemingly stable system into the unstable regime. Furthermore, we explored the boundaries of this regime for different TTI strategies and efficiencies of the TTI implementation.

Our results are in agreement with other simulation and modeling studies investigating how efficient TTI strategies are in curbing the spread of the SARS-CoV-2. Both agent-based studies with realistic contact structures [4] and studies using mean-field spreading dynamics with tractable equations [29, 30] agree that TTI measures are an important contribution to control the pandemic. Fast isolation is arguably the most crucial factor, which is included in our model in the testing rate λ_s. Yet, TTI is generally not perfect and the app-based solutions that have been proposed at present still lack the necessary large adoption that was initially foreseen, and that is necessary for these solutions to work [30]. Our work as well as others [4, 30–32] show that realistic TTI can compensate reproduction numbers of around 1.5-2.5, which is however lower than the base reproduction number of around 3.3. This calls for continued contact reduction on the order of 25–55 %, and it does not only highlight the importance of TTI, but also the need of other mitigation measures.

Our work extends previous studies by combining the explicit modeling of a hidden pool (including test avoiders) with the exploration of various ways of allocating testing and tracing resources. This allows us to investigate the effectiveness of various approaches to stabilize disease dynamics in the face of a relaxation of physical distancing. This yields important insights for policy makers into how to allocate resources. We also include a capacity limit of tracing, which is typically not included in other studies, but important to understand the meta-stable regime of a TTI-stabilized system, and to understand the importance of keeping a safety distance to the critical reproduction number of a given TTI strategy. Last, we highlight the important differences between the observed reproduction numbers — as they are reported in the media — and the more important, but hard to access, reproduction number in the hidden pool. Specifically we show how transient behavior of the observed reproduction number may be easily misinterpreted.

Limited TTI capacity implies a meta-stable regime with the risk of sudden explosive growth. Both, testing as well as tracing contribute to containing the spread of SARS-CoV-2. However, if their capacity limit is exceeded by the number of new infections, then an otherwise controlled spread becomes uncontrolled. This is particularly troubling, because the spread is self-accelerating: the more the capacity limit is exceeded, the less the testing and tracing can contribute to containment. To avoid this situation, the reproduction number has to stay below its critical value, *and* the number of new infections below TTI capacity. Therefore, it is advisable to maintain a safety margin to these limits. Otherwise, a small increase of the reproduction number, super-spreading events [33], or sudden influx of new cases e.g. after holidays, lead to uncontrolled spread. Re-establishing stability is then quite difficult.

The relative efficiencies of random, symptom-driven and tracing-based testing should determine the allocation of resources. As the number of available tests is limited, a decision on how to distribute these tests across the different strategies is important. In general, the more COVID-19 cases are detected by the given number of tests, the more efficient their use is. Thus, the efficiency of test strategies in terms of positive rate is a primary metric to determine the allocation of tests. Yet, in some situations special considerations apply, and we will discuss those below.

Testing the persons identified by contact tracing is the most efficient strategy under conditions of low prevalence. Here, the expected fraction of positive tests is R_t^H divided by the average number of traced contacts. If we consider an average number of contacts of 30, combined with a tracing efficiency of 0.66, we obtain an estimate for the efficiency of tracing based testing of $R_t^H \cdot \eta / 30 \cdot \eta \approx 1/15$ for an R_t^H of 2. In other words, to detect a case of SARS-CoV-2 infection, 15 tests have to be invested. This relatively high efficiency of contact-tracing based tests also suggests that contacts should isolate immediately after being identified as a contact, not only after receiving a positive test. In fact, testing maybe slightly delayed in identified and isolated contacts — to make sure these contacts are past their incubation period. Otherwise, false negative results will lead to behavior enabling further disease spread.

For the efficiency of symptom-driven testing a similar estimate is much harder to obtain, and depends strongly on which symptoms are included in the recommendations for testing. This is because symptoms of COVID-19 like fever and cough are unfortunately shared with other common respiratory infections; furthermore, in children respiratory symptoms are usually less severe, and gastrointestinal symptoms may also be present [34]— widening the array of symptoms that may indicate an infection with SARS-CoV-2. Thus, diseases like common cold can produce an enormous number of individuals with symptoms, but not SARS-CoV-2 infections, that may have to be included in testing. Realistically, the current efficiency of symptom-driven testing might be close to the fraction of SARS-CoV-2 cases among all influenza-like cases, which is currently around 4% [35], but will depend on influenza-seasonality and SARS-CoV-2 prevalence. However, if less specific symptoms are also accounted for, the efficiency would currently be lower, probably close to the current rate of positive tests in general. This means that roughly 25-100 symptom-driven tests may have to be administered for one positive result at present. Therefore, symptom-driven testing is potentially less efficient than tests based on contact tracing. Using a narrower set of symptoms for admission to COVID-19 testing will increase efficiencies, but will inevitably increase the effective fraction of asymptomatic persons (ξ^{ap} in our model). As an example, the loss of smell or taste is a COVID-19 symptom [14,36,37] that has proven to be highly specific (when combined with fever) in a recent prospective study [38]. However, allowing only individuals with this symptom combination for testing will cover less than 67% of the symptomatic infected individuals ([38], Suppl. Table 1 therein). This leads to a rather large value for ξ^{ap}, as those with the "wrong" symptoms are then considered asymptomatic. Another important point to consider is that a moderate increase in λ_s may be obtained with few additional tests (and a better organization of the test pipeline), but a larger increase may require a strong relaxation of criteria for test admission, so that people can get tested earlier. This in turn may lead to an excessive increase in symptom-driven test numbers. The efficiency of symptom-driven testing is improved directly by hygiene and remaining physical distancing measures via easing the test-load created by symptomatic carriers of other infections. Vaccination against influenza, for example, also falls into this category of measures that reduce testing load. When authorities, however, rely mostly on testing and contact tracing without any flanking physical distancing and hygiene regulations other infectious diseases with COVID-19 like symptoms become a major concern.

In random testing, the efficiency of detecting SARS-CoV-2 infections is governed by the prevalence of the infection in the general population. As long as this prevalence is low, a random test has a very low probability to detect an infection. Thus, random testing should be reserved for specific scenarios, such as the protection of communities where no infection must enter, e.g. nursing homes and hospitals, or communities with high prevalence, i.e. those with locally clustered outbreaks.

In sum, our results suggest that testing capacities should be focused on testing traced contacts of infected individuals, and on symptom-driven testing. Random testing seems to be useful only to protect particularly vulnerable communities or around local hot spots of infections. Another use of random testing is to provide some information about the current prevalence of the disease, and to facilitate estimates of the reproduction number in the hidden pool R_t^H, which remains nevertheless difficult to estimate.

The cooperation of the general population in maintaining a low reproduction number is essential even with efficient TTI strategies in place. Our results illustrate that the reproduction number in the hidden pool R_t^H — which reflects the public's behavior — is still central to disease control. Specifically, we found that $R_t^H \leq 1.4$ (95 % CI, 1.23–1.69) can very likely be compensated by testing and isolating alone,

whereas additional contract tracing shifts this boundary to $R_t^H \leq 1.9$ (95 % CI, 1.42–2.70, Fig. S2, Tab. S1). Both of these values are substantially lower than the basic reproduction number of SARS-CoV-2, $R_0 \approx 3.3$. Thus, if the goal is to contain the spread of SARS-CoV-2 with the available TTI-related resources, the reproduction number in the hidden pool will have to be reduced effectively by roughly $25 - 55\%$ compared to the beginning of the pandemic. This effective reduction may be achieved by a suitable combination of hygiene measures, such as mask wearing, filtering or exchange of contaminated air, and physical distancing. Useful accompanying measures on a voluntary basis include: immediately and strictly self-isolating upon any symptoms compatible with COVID-19, avoiding travel to any region with a higher infection rate, keeping a personal contact diary, using the digital tracing app, selecting only those contacts that are essential for one's well being, and avoiding contacts inside closed rooms if possible. Most of these measures and also an efficient tracing cannot be achieved without widespread cooperation of the population. This cooperation might be increased by a ramping up of coordinated educational efforts around explaining mechanisms and dynamics of disease spreading to a broad audience — instead of just providing behavioral advice.

Conclusion Based on a simulation of disease dynamics influenced by realistic TTI strategies with parameters taken from the example of Germany, we show that the spreading dynamics of SARS-CoV-2 can only be stabilized if effective TTI-strategies are combined with hygiene and physical distancing measures that keep the reproduction number in the general population below a value of approximately $R_t^H \leq 1.9$ (95 % CI, 1.42–2.70). As a system stabilized by TTI with a finite capacity is only in a meta-stable state and can be tipped into instability by one-time effects, it would be desirable to keep a safety distance even to these values, if possible. The above bounds on the reproduction number in the hidden pool can be easily recomputed for other countries with different TTI capacities and reproduction numbers.

Methods

We model the spreading dynamics of SARS-CoV-2 as the sum of contributions from two pools, i.e. traced T and hidden H infections (see sketch in Fig. 2). The first pool (T) contains traced cases revealed through testing or by contact tracing of an individual that has already been tested positive; all individuals in the traced pool are assumed to isolate themselves (quarantine), avoiding further contacts as well as possible. In contrast, in the second pool, infections spread silently, and only become detected when individuals develop symptoms and get tested, or via random testing in the population. This second pool (H) is therefore called the hidden pool H; individuals in this pool are assumed to exhibit the behavior of the general population, thus of anyone who is not aware of being infected. We model the mean-field interactions between the hidden and the traced pool, and distinguish between symptomatic and asymptomatic carriers. This is central when exploring different testing strategies (as detailed below). We also include effects of non-compliance and imperfect contact tracing, as well as a non-zero influx Φ of new cases entering from outside. As this influx makes an eradication of SARS-CoV-2 impossible, only an exponential growth of cases or a stable rate of new infections are possible modeling outcomes. Therefore, we frame our investigation as a stability problem, where the aim is to implement test-trace-and-isolate strategies in a way that allows the system to remain stable.

Spreading Dynamics

Concretely, we use a modified SIR-type model, where infections I are either symptomatic (I^s) or asymptomatic (I^a), and they belong to the hidden (H) or a traced (T) pool of infections (Fig. 2), thus creating in total four compartments of infections (H^s, H^a, T^s, T^a). New infections are asymptomatic with a ratio ξ^{ap}, the others are symptomatic. In all compartments individuals are removed with a rate Γ because of recovery or death (see Tab. 1 for all parameters).

In the hidden pool, the disease spreads according to the reproduction number R_t^H. This reproduction number reflects the disease spread in the general population, without testing induced isolation of individuals. In addition, the hidden pool receives a mobility-induced influx Φ of new infections. Cases are removed from the hidden pool (i) when detected by TTI, and put into the traced pool, or (ii) due to recovery or death.

The traced pool T contains those infected individuals who have been tested positive as well as their positively tested contacts. As these individuals are (imperfectly) isolated, their reproduction number R_t^H is multiplied by an isolation factor ν within the traced pool. We assume that they mainly spread infections to known contacts, however, we also assume that some contacts of these isolated are missed, causing a leak ϵ of infections into the hidden pool. The reproduction number of the traced pool therefore is defined as: $R_t^T = (\nu + \epsilon) R_t^H$.

Within our model, we concentrate on the case of low incidence and low fraction of immune people, as in any new outbreak or for disease with quickly waning immunity [39]. Our model can also reflect innate or acquired immunity; one then has to rescale the population or the reproduction number. The qualitative behavior of the dynamics is not expected to change.

Parameter Choices and Scenarios

For any testing strategy, the fraction of infections that do not develop any symptoms across the whole infection timeline is an important parameter, and this also holds for testing strategies applied to the case of SARS-CoV-2. In our model this parameter is called ξ^{ap} and includes beside true asymptomatic infections ξ also the fraction of individuals that avoid testing φ.

The exact value of the fraction of asymptomatic infections ξ, however, is still fraught with uncertainty, and it also depends on age [14, 40, 41]. While early estimates were as high as 50 % (for example ranging from 26 % to 63 % [42]), these early estimates suffered from reporting bias, small sample sizes and sometimes included pre-symptomatic cases as well [21, 43]. Recent bias-corrected estimates from large sample sizes range between 12 % [21] and 33 % [22]. We decided to use 15 % for the pure asymptomatic ratio ξ.

In addition, we include a fraction φ of individuals avoiding testing. This can occur because individuals do not want to be in contact with governmental authorities or because they deem risking a spread of SARS-CoV-2 less important than having to quarantine [15]. As this part of the population may act in the same manner as asymptomatic persons, we include it in the asymptomatic compartment of the hidden pool, assuming a value of 0.2. We thus arrive at an effective ratio of asymptomatic infections $\xi^{\mathrm{ap}} = \xi + (1 - \xi)\varphi = 0.32$. We assume that both, symptomatic and asymptomatic persons, have the same reproduction number.

In general, infected individuals move from the hidden to the traced pool after being tested; yet, also a small number of infections will leak from the traced to the hidden pool with rate $\epsilon \Gamma R_t^H$, with $\epsilon = 0.1$. A source of leak would be a contact that has been infected, traced and tested positive, but still ignores quarantine instructions. For the model, this individual has the same effect on disease dynamics as someone from the hidden pool.

Another crucial parameter for any TTI strategy is the reproduction number in the hidden pool R_t^H. This parameter is by definition impossible to measure, but it presents typically the main driver of the spreading dynamics. It depends mainly on the contact behavior of the population, and ranges from R_0 in the absence of contact restrictions to values below 1 during strict lock-down [2]. For the default parameters of our model, we used a value of $R_t^H = 1.8$. This value causes new infections to be approximately constant. A constant number of new infections was observed for Germany during much of summer 2020 [44]. This value of $R_t^H = 1.8$ is about 54 % lower than the basic reproduction number $R_0 \approx 3.3$, hence we assume that some non-pharmacological interventions (physical distancing or hygiene measures) [1, 2] are in place. For additional scenarios, we explored the impact of both higher and lower values of R_t^H on our TTI strategy.

Testing-and-Tracing strategies

We consider three different testing-and-tracing strategies: random testing, symptom-driven testing and specific testing of traced contacts. Despite the naming — chosen to be consistent with existing literature [4, 45–48]— an isolation of the cases tested positive is part of all of these strategies. The main differences lie in whom the tests are applied to and whether past contacts of an infected person are traced and told to isolate. Our model simulates the parallel application of all three strategies – as it is typical for real-world settings, and yields the effects of the "pure" application of these strategies as corner cases realized via specific parameter settings.

Random testing is defined here as applying tests to individuals irrespective of their symptom status, or whether they belonging to the contact-chain of other infected individuals. In our model, random testing transfers infected individuals from the hidden to the traced pool with fixed rate λ_r, irrespective of them showing symptoms or not. In reality, random testing is often implemented as situation-based testing for a sub-group of the population, e.g. at a hot-spot, for groups at risk, or for people returning from travel. Such situation-based strategies would be more efficient than the random testing assumed in this model. Nonetheless, because random testing can detect symptomatic and asymptomatic persons alike, we decided to evaluate its potential contribution to contain the spread.

The number of random tests that can be performed is limited by the available laboratory and sample collection capacity. For orientation, we included therefore a maximal testing capacity of $\lambda_{r,\mathrm{max}} = 0.002$ test per person and day, which reflects the laboratory capacity in Germany (1.2 Mio. per week) [44, 49]. Potentially, the

testing capacity can be increased by pooling PCR-tests, without strongly reducing the sensitivity [23]. We acknowledge this possibility by also taking into account a ten times larges testing capacity, $10 \cdot \lambda_{r,\max} = 0.02$. This would correspond to every person being tested on average every 50 days (7 weeks) - summing to about 12 Mio. tests per week in Germany.

Symptom-driven testing is defined as applying tests to individuals presenting symptoms of COVID-19. In this context, it is important to note that non-infected individuals can have symptoms similar to those of COVID-19, as many symptoms are rather unspecific. Although symptom-driven testing suffers less from imperfect specificity, it can only uncover symptomatic cases that are willing to be tested (see below). Here, *symptomatic infected individuals* are transferred from the hidden to the traced pool at rate λ_s.

We define λ_s as the rate at which a symptomatic infected individual gets tested per day. As default value we use $\lambda_s = 0.1$, which means that one in ten people that show symptoms gets tested each day and are subsequently isolated. In principle this rate could be increased to 1, reflecting that a symptomatic person is tested and isolated after one day. For SARS-CoV-2, such a fast detection is unrealistic, because typically infected people show a the delay of 1-2 days between the beginning of infectiousness and showing symptoms [50]. Hence, $\lambda_s \approx 0.5$ is an upper limit to the symptom-driven testing rate.

Tracing contacts of positively tested individuals presents a very specific test strategy, and is expected to be effective in breaking the infection chains, if contacts self-isolate sufficiently quickly [4, 45, 51]. However as every implementation of a TTI strategy is bound to be imperfect, we assume that only a fraction $\eta < 1$ of all contacts can be traced. These contacts, if tested positive, are then transferred from the hidden to the traced pool. We assumed a default value of $\eta = 0.66$, i.e. on average two thirds of the contacts are identified.

Contact tracing is mainly done by the health authorities in Germany, and this clearly limits the maximum number $N_{\max}$ of observed new cases $\hat{N}^{\mathrm{obs}}$, for which contact tracing is still functional. In the first part of the manuscript, we assume for simplicity that $\hat{N}^{\mathrm{obs}}$ is sufficiently small to not exceed the tracing capacity; in the second part, we explicitly explore the role of this limit.

In principle, the tracing capacity limit can be expressed in two ways, either as the number of observed cases $\hat{N}^{\mathrm{obs}}$, at which tracing starts to break down (denoted by $N_{\max}$), or as number of positive contacts that can maximally be detected and handled on average by the health departments ($n_{\max}$). Both values obviously depend strongly on the TTI scenario, the population's behavior, and the health departments. As default value, we assume $N_{\max} = 675$. This corresponds to uncovering $n_{\max} = 300$ positive contact persons by testing and tracing from the *hidden* pool (in the default scenario). The other about 375 persons originate within the traced pool (e.g. infected family members), and are therefore considered to be detected with much less effort. The limit of $n_{\max} = 300$ is currently well within reach of the 400 health departments in Germany. At first sight, this limit may appear low (about one case per working day per health department). However, identifying, contacting and counselling all contact persons (thus many more persons than 300), and finally testing them and controlling their quarantine requires considerable effort.

Any testing can in principle produce both false-positive (quarantined individuals who were not infected) and false-negative (non-quarantined infected individuals) cases. False-positive rates in theory should be very low (0.2 % or less for RT-PCR tests). However, testing and handling of the probes can induce false-positive results [52–55]. Under low prevalence of SARS-CoV-2, false-positive could therefore outweigh true-positive, especially for the random testing strategy, where the number of tests required to detect new infections would be very high [39, 56]. This should be carefully considered when choosing an appropriate testing strategy, but has not explicitly modeled here, as it does not contribute strongly to whether or not the outbreak could be controlled.

Model Equations

The contributions of the spreading dynamics and the TTI strategies are summarized in the equations below. They govern the spreading dynamics of case numbers in and between the hidden and the traced pool, H and T. We assume a regime of low prevalence and low immunity, i.e. the majority of the population is susceptible. Thus, the dynamics are completely determined by spread (characterized by the reproduction numbers R_t), recovery (characterized by the recovery rate Γ), external influx Φ and the impact of the TTI strategies:

$$\frac{dT}{dt} = \underbrace{\Gamma\left(\nu R_t^H - 1\right)T}_{\text{spreading dynamics}} \quad \underbrace{+\,\lambda_s H^s + \lambda_r H}_{\text{testing}} + \underbrace{f\left(H^s, H\right)}_{\text{tracing}}, \tag{1}$$

$$\frac{dH}{dt} = \underbrace{\Gamma\left(R_t^H - 1\right)H}_{\text{spreading dynamics}} \quad \underbrace{-\left(\lambda_s H^s + \lambda_r H\right)}_{\text{testing}} \underbrace{-\,f\left(H^s, H\right)}_{\text{tracing}} + \underbrace{\Gamma\epsilon R_t^H T}_{\text{missed contacts}} + \underbrace{\Phi}_{\text{external influx}}, \tag{2}$$

$$\frac{1}{1-\xi^{\mathrm{ap}}}\frac{dH^s}{dt} = \underbrace{\Gamma\left(R_t^H H - \frac{H^s}{1-\xi^{\mathrm{ap}}}\right)}_{\text{spreading dynamics}} \underbrace{-\frac{\left(\lambda_s + \lambda_r\right)H^s}{1-\xi^{\mathrm{ap}}}}_{\text{testing}} \underbrace{-\,f\left(H^s, H\right)}_{\text{tracing}} + \underbrace{\Gamma\epsilon R_t^H T}_{\text{missed contacts}} + \underbrace{\Phi}_{\text{external influx}}, \tag{3}$$

$$H^a = H - H^s, \tag{4}$$

$$\text{with } f(H^s, H) = \min\left\{n_{\max}, \eta R_t^H\left(\lambda_s H^s + \lambda_r H\right)\right\}. \tag{5}$$

Equations (1) and (2) describe the dynamical evolution of both the traced and hidden pools. They are however not sufficient to completely describe the underlying dynamics of the system in the hidden pool, as the symptomatic and asymptomatic subpools behaves slightly different: only from the symptomatic hidden pool (H^s) cases can be removed because of symptom-driven testing. Thus the specific dynamics of H^s is defined by equation (3). The dynamics of the asymptomatic hidden pool (H^a) can be inferred from equation (4). In the traced compartment, the asymptomatic and symptomatic pools do not need to be distinguished, as their behavior is assumed to be identical. Equation (5) reflects a potential limit $n_{\max}$ of the tracing capacity of the health authorities. It is expressed as the total number of positive cases that can be detected from tracing the contacts of people who were detected via symptom-driven testing (from H^s) or via random testing (from H).

Central epidemiological parameters that can be observed

In the real world, the disease spread can only be observed by the traced pool. While the *true* number of daily infections N is a sum of all new infections in the hidden and traced pools, the *observed* number of daily infections $\hat{N}^{\mathrm{obs}}$ is the number of new infections in the traced pool delayed by a variable reporting delay α. This includes internal contributions and contributions from testing and tracing:

$$N(t) = \underbrace{\Gamma R_t^T T(t)}_{\text{traced pool}} + \underbrace{\Gamma R_t^H H(t)}_{\text{hidden pool}} + \underbrace{\Phi}_{\text{external influx}} \tag{6}$$

$$\hat{N}^{\mathrm{obs}}(t) = \left[\underbrace{\Gamma\nu R_t^H T(t)}_{\text{traced pool}} + \underbrace{\lambda_s H^s(t) + \lambda_r H(t)}_{\text{testing}} + \underbrace{f(H^s(t), H(t))}_{\text{tracing}}\right] \circledast \mathcal{G}[\alpha = 4, \beta = 1](t), \tag{7}$$

where $f(H^s, H)$ is defined in (5), $\circledast$ denotes a convolution and $\mathcal{G}$ a Gamma distribution that models a variable reporting delay. The spreading dynamics are usually characterized by the observed reproduction number $\hat{R}_t^{\mathrm{obs}}$, which is calculated from the observed number of new cases $\hat{N}^{\mathrm{obs}}(t)$. We here use the definition underlying the estimates that are published by Robert-Koch-Institute, the official body responsible for epidemiological control in Germany [57]: the reproduction number is the relative change of daily new cases N separated by 4 days (the assumed serial interval of COVID-19 [58]):

$$\hat{R}_t^{\mathrm{obs}} = \frac{\hat{N}^{\mathrm{obs}}(t)}{\hat{N}^{\mathrm{obs}}(t-4)} \tag{8}$$

$$\hat{R}_t^{\mathrm{eff}} = \frac{N(t)}{N(t-4)} \tag{9}$$

While only $\hat{R}_t^{\mathrm{obs}}$ is accessible from the observed new cases, in the model one can also define an effective reproduction number $\hat{R}_t^{\mathrm{eff}}$ from the total number of daily new infections.

In contrast to the original definition of $\hat{R}_t^{\mathrm{obs}}$ [57], we do not need to remove real-world noise effects by smoothing this ratio.

Numerical calculation of solutions and critical values.

The numerical solution of the differential equations governing our model were obtained using a versatile solver based on an explicit Runge-Kutta (4,5) formula, `@ode45`, implemented in MATLAB (version 2020a), with default settings. This algorithm allows the solution of non-stiff systems of differential equations in the shape $y' = f(t, y)$, given a user-defined time-step (for us, 0.1 days). Suitability and details on the algorithm are further discussed in [59].

To derive the tipping point between controlled and uncontrolled outbreaks (e.g. critical values of R_t^H), and to plot the stability diagrams, we used the `@fzero` MATLAB function. This function uses a combination of bisection, secant, and inverse quadratic interpolation methods to find the roots of a functions. For instance, following the discussion of Section , R_{crit}^H was determined by finding the roots of the function returning the real part of the linear system's largest eigenvalue.

Table 1: Model parameters.

Parameter	Meaning	Value (default)	Range	Units	Source
M	Population size	80 000 000		people	Assumed
R_0	Basic reproduction number	3.3	2.2–4.4	–	$[20, 60, 61]^1$
R_t^H	Reproduction number (hidden)	1.80		–	$[2, 62, 63]$
Γ	Recovery rate	0.10	0.08–0.12	day^{-1}	$[50, 64$–$66]$
ξ	Asymptomatic ratio	0.15	0.12–0.33	–	$[21, 22]$
φ	Fraction skipping testing	0.20	0.10–0.40	–	$[15]$
ν	Isolation factor (traced)	0.10		–	Assumed
λ_r	random-testing rate	0	0–0.02	day^{-1}	Assumed
λ_s	symptom-driven testing rate	0.10	0–1	day^{-1}	Assumed
η	Tracing efficiency	0.66		–	Assumed
N_{max}	Maximal tracing capacity	≈ 675	200–6000	$\mathrm{cases\,day}^{-1}$	Assumed^2
ϵ	Missed contacts (traced)	0.10		–	Assumed
Φ	Influx rate (hidden)	15		$\mathrm{cases\,day}^{-1}$	Assumed^2
$\lambda_{r,\mathrm{max}}$	Maximal test capacity per capita	0.002		$\mathrm{cases\,day}^{-1}$	$[44, 49]$
R_t^T	Reproduction number (traced)	0.36		–	$R_t^T = (\nu + \epsilon)\, R_t^H$
ξ^{ap}	Apparent asymptomatic ratio	0.32		–	$\xi^{\mathrm{ap}} = \xi + (1 - \xi)\varphi$
R_{crit}^H	Critical reproduction number (hidden)	1.89		–	Numerically calculated from model parameters

^{1}This value may depend on cultural and social factors as well as on the estimation methodology.
^{2}Chosen for a country with a population of $M = 80 \cdot 10^6$. See methods for considerations.

Acknowledgments

Table 2: Model variables.

Variable	Meaning	Units	Explanation
H^a	Hidden asymptomatic pool	people	Non-traced, non-isolated people who are asymptomatic or avoid being tested
H^s	Hidden symptomatic pool	people	Non-traced, non-isolated people who are symptomatic
T^a	Traced asymptomatic pool	people	Traced (isolated) people who are asymptomatic
T^s	Traced symptomatic pool	people	Traced (isolated) people who are symptomatic
H	Hidden pool	people	Total non-traced people: $H = H^a + H^s$
T	Traced pool	people	Total traced people: $T = T^a + T^s$
N	New infections (traced and hidden)	cases day^{-1}	Given by: $N = \Gamma R_t^T T + \Gamma R_t^H H + \Phi$
$\hat{N}^{\mathrm{obs}}$	Observed new infections (influx to traced pool)	cases day^{-1}	Only cases of the traced pool; delayed on average by 4 days because of reporting
$\hat{R}_t^{\mathrm{eff}}$	Estimated effective reproduction number	–	Estimated from the cases of all pools: $\hat{R}_t^{\mathrm{eff}} = N(t)/N(t-4)$
$\hat{R}_t^{\mathrm{obs}}$	Observed reproduction number	–	The reproduction number that can be estimated only from the observed cases: $\hat{R}_t^{\mathrm{obs}} = \hat{N}^{\mathrm{obs}}(t)/\hat{N}^{\mathrm{obs}}(t-4)$

References

[1] Jan Markus Brauner, Mrinank Sharma, Sören Mindermann, Anna B Stephenson, Tomáš Gavenčiak, David Johnston, John Salvatier, Gavin Leech, Tamay Besiroglu, George Altman, et al. The effectiveness and perceived burden of nonpharmaceutical interventions against COVID-19 transmission: a modelling study with 41 countries. *medRxiv*, 2020.

[2] Jonas Dehning, Johannes Zierenberg, F Paul Spitzner, Michael Wibral, Joao Pinheiro Neto, Michael Wilczek, and Viola Priesemann. Inferring change points in the spread of COVID-19 reveals the effectiveness of interventions. *Science*, 2020.

[3] Marcel Salathé, Christian L Althaus, Richard Neher, Silvia Stringhini, Emma Hodcroft, Jacques Fellay, Marcel Zwahlen, Gabriela Senti, Manuel Battegay, Annelies Wilder-Smith, et al. COVID-19 epidemic in switzerland: on the importance of testing, contact tracing and isolation. *Swiss medical weekly*, 150(11-12):w20225, 2020.

[4] Adam J Kucharski, Petra Klepac, Andrew Conlan, Stephen M Kissler, Maria Tang, Hannah Fry, Julia Gog, John Edmunds, CMMID COVID-19 Working Group, et al. Effectiveness of isolation, testing, contact tracing, and physical distancing on reducing transmission of SARS-CoV-2 in different settings: a mathematical modelling study. *The Lancet Infectious Diseases*, 0(0), June 2020.

[5] Nick Warren Ruktanonchai, JR Floyd, Shengjie Lai, Corrine Warren Ruktanonchai, Adam Sadilek, Pedro Rente-Lourenco, Xue Ben, Alessandra Carioli, Joshua Gwinn, JE Steele, et al. Assessing the impact of coordinated COVID-19 exit strategies across Europe. *Science*, 2020.

[6] Vernon J Lee, Calvin J Chiew, and Wei Xin Khong. Interrupting transmission of COVID-19: lessons from containment efforts in Singapore. *Journal of Travel Medicine*, 27(3):taaa039, 2020.

[7] Rachael Pung, Calvin J Chiew, Barnaby E Young, Sarah Chin, Mark IC Chen, Hannah E Clapham, Alex R Cook, Sebastian Maurer-Stroh, Matthias PHS Toh, Cuiqin Poh, et al. Investigation of three clusters of COVID-19 in Singapore: implications for surveillance and response measures. *The Lancet*, 2020.

[8] JaHyun Kang, Yun Young Jang, Jinwha Kim, Si-Hyeon Han, Ki Rog Lee, Mukju Kim, and Joong Sik Eom. South Korea's reponses to stop the COVID-19 pandemic. *American Journal of Infection Control*, 2020.

[9] Ezekiel J Emanuel, Govind Persad, Ross Upshur, Beatriz Thome, Michael Parker, Aaron Glickman, Cathy Zhang, Connor Boyle, Maxwell Smith, and James P Phillips. Fair allocation of scarce medical resources in the time of COVID-19, 2020.

[10] Guanjian Li, Weiran Li, Xiaojin He, and Yunxia Cao. Asymptomatic and presymptomatic infectors: hidden sources of COVID-19 disease. *Clinical Infectious Diseases: An Official Publication of the Infectious Diseases Society of America*, 2020.

[11] Feng Ye, Shicai Xu, Zhihua Rong, Ronghua Xu, Xiaowei Liu, Pingfu Deng, Hai Liu, and Xuejun Xu. Delivery of infection from asymptomatic carriers of COVID-19 in a familial cluster. *International Journal of Infectious Diseases*, 2020.

[12] Mirjam Kretzschmar, Ganna Rozhnova, and Michiel van Boven. Effectiveness of isolation and contact tracing for containment and slowing down a COVID-19 epidemic: a modelling study. *Available at SSRN 3551343*, 2020.

[13] Camilla Rothe, Mirjam Schunk, Peter Sothmann, Gisela Bretzel, Guenter Froeschl, Claudia Wallrauch, Thorbjörn Zimmer, Verena Thiel, Christian Janke, Wolfgang Guggemos, et al. Transmission of 2019-nCoV infection from an asymptomatic contact in Germany. *New England Journal of Medicine*, 382(10):970–971, 2020.

[14] Chih-Cheng Lai, Yen Hung Liu, Cheng-Yi Wang, Ya-Hui Wang, Shun-Chung Hsueh, Muh-Yen Yen, Wen-Chien Ko, and Po-Ren Hsueh. Asymptomatic carrier state, acute respiratory disease, and pneumonia due to severe acute respiratory syndrome coronavirus 2 (SARS-CoV-2): facts and myths. *Journal of Microbiology, Immunology and Infection*, 2020.

[15] John H McDermott and William G Newman. Refusal of viral testing during the SARS-CoV-2 pandemic. *Clinical Medicine*, 2020.

[16] Kevin Linka, Proton Rahman, Alain Goriely, and Ellen Kuhl. Is it safe to lift COVID-19 travel bans? the newfoundland story. *medRxiv*, 2020.

[17] Jasmina Panovska-Griffiths, Cliff Kerr, Robyn Margaret Stuart, Dina Mistry, Daniel Klein, Russell M Viner, and Chris Bonell. Determining the optimal strategy for reopening schools, work and society in the UK: balancing earlier opening and the impact of test and trace strategies with the risk of occurrence of a secondary COVID-19 pandemic wave. *medRxiv*, 2020.

[18] William Ogilvy Kermack and Anderson G McKendrick. A contribution to the mathematical theory of epidemics. *Proceedings of the royal society of london. Series A, Containing papers of a mathematical and physical character*, 115(772):700–721, 1927.

[19] Herbert W Hethcote. An immunization model for a heterogeneous population. *Theoretical population biology*, 14(3):338–349, 1978.

[20] Ying Liu, Albert A Gayle, Annelies Wilder-Smith, and Joacim Rocklöv. The reproductive number of COVID-19 is higher compared to SARS coronavirus. *Journal of travel medicine*, 2020.

[21] Oyungerel Byambasuren, Magnolia Cardona, Katy Bell, Justin Clark, Mary-Louise McLaws, and Paul Glasziou. Estimating the extent of true asymptomatic COVID-19 and its potential for community transmission: systematic review and meta-analysis. *Available at SSRN 3586675*, 2020.

[22] Marina Pollán, Beatriz Pérez-Gómez, Roberto Pastor-Barriuso, Jesús Oteo, Miguel A Hernán, Mayte Pérez-Olmeda, Jose L Sanmartín, Aurora Fernández-García, Israel Cruz, Nerea Fernández de Larrea, et al. Prevalence of SARS-CoV-2 in spain (ENE-COVID): a nationwide, population-based seroepidemiological study. *The Lancet*, 2020.

[23] Stefan Lohse, Thorsten Pfuhl, Barbara Berkó-Göttel, Jürgen Rissland, Tobias Geißler, Barbara Gärtner, Sören L. Becker, Sophie Schneitler, and Sigrun Smola. Pooling of samples for testing for SARS-CoV-2 in asymptomatic people. *The Lancet Infectious Diseases*, 0(0), April 2020.

[24] Giovanni Bonaccorsi, Francesco Pierri, Matteo Cinelli, Andrea Flori, Alessandro Galeazzi, Francesco Porcelli, Ana Lucia Schmidt, Carlo Michele Valensise, Antonio Scala, Walter Quattrociocchi, et al. Economic and social consequences of human mobility restrictions under COVID-19. *Proceedings of the National Academy of Sciences*, 117(27):15530–15535, 2020.

[25] Robert Rowthorn and Jan Maciejowski. A cost-benefit analysis of the COVID-19 disease. *Oxford Review of Economic Policy*, 2020.

[26] Cliff C Kerr, Robyn M Stuart, Dina Mistry, Romesh G Abeysuriya, Gregory Hart, Katherine Rosenfeld, Prashanth Selvaraj, Rafael C Nunez, Brittany Hagedorn, Lauren George, et al. Covasim: an agent-based model of COVID-19 dynamics and interventions. *medRxiv*, 2020.

[27] Masoud Jalayer, Carlotta Orsenigo, and Carlo Vercellis. CoV-ABM: A stochastic discrete-event agent-based framework to simulate spatiotemporal dynamics of COVID-19. *arXiv preprint arXiv:2007.13231*, 2020.

[28] Sandro Meloni, Nicola Perra, Alex Arenas, Sergio Gómez, Yamir Moreno, and Alessandro Vespignani. Modeling human mobility responses to the large-scale spreading of infectious diseases. *Scientific reports*, 1:62, 2011.

[29] Christophe Fraser, Steven Riley, Roy M Anderson, and Neil M Ferguson. Factors that make an infectious disease outbreak controllable. *Proceedings of the National Academy of Sciences*, 101(16):6146–6151, 2004.

[30] Luca Ferretti, Chris Wymant, Michelle Kendall, Lele Zhao, Anel Nurtay, Lucie Abeler-Dörner, Michael Parker, David Bonsall, and Christophe Fraser. Quantifying SARS-CoV-2 transmission suggests epidemic control with digital contact tracing. *Science*, 368(6491), 2020.

[31] Joel Hellewell, Sam Abbott, Amy Gimma, Nikos I Bosse, Christopher I Jarvis, Timothy W Russell, James D Munday, Adam J Kucharski, W John Edmunds, Fiona Sun, et al. Feasibility of controlling COVID-19 outbreaks by isolation of cases and contacts. *The Lancet Global Health*, 2020.

[32] Emma L Davis, Tim CD Lucas, Anna Borlase, Timothy M Pollington, Sam Abbott, Diepreye Ayabina, Thomas Crellen, Joel Hellewell, Li Pi, Graham F Medley, et al. An imperfect tool: COVID-19'test & trace' success relies on minimising the impact of false negatives and continuation of physical distancing. *medRxiv*, 2020.

[33] Benjamin M Althouse, Edward A Wenger, Joel C Miller, Samuel V Scarpino, Antoine Allard, Laurent Hébert-Dufresne, and Hao Hu. Stochasticity and heterogeneity in the transmission dynamics of SARS-CoV-2. *arXiv preprint arXiv:2005.13689*, 2020.

[34] Petra Zimmermann and Nigel Curtis. Coronavirus infections in children including COVID-19: an overview of the epidemiology, clinical features, diagnosis, treatment and prevention options in children. *The Pediatric infectious disease journal*, 39(5):355, 2020.

[35] Arbeitsgemeinschaft Influenza. Influenza-Monatsbericht. `https://influenza.rki.de/Wochenberichte/2019_2020/2020-32.pdf`, 2020. Accessed: 2020-08-27.

[36] Carol H. Yan, Farhoud Faraji, Divya P. Prajapati, Christine E. Boone, and Adam S. DeConde. Association of chemosensory dysfunction and COVID-19 in patients presenting with influenza-like symptoms. *International Forum of Allergy & Rhinology*, 10(7):806–813, 2020.

[37] Cristina Menni, Ana Valdes, Maxim B Freydin, Sajaysurya Ganesh, Julia El-Sayed Moustafa, Alessia Visconti, Pirro Hysi, Ruth C E Bowyer, Massimo Mangino, Mario Falchi, Jonathan Wolf, Claire Steves, and Tim Spector. Loss of smell and taste in combination with other symptoms is a strong predictor of COVID-19 infection. *medRxiv*, 2020.

[38] Alan Chen, Amol Agarwal, Nishal Ravindran, Chau To, Talan Zhang, and Paul J. Thuluvath. Are Gastrointestinal Symptoms Specific for Coronavirus 2019 Infection? A Prospective Case-Control Study From the United States. *Gastroenterology*, 0(0), May 2020.

[39] Robert D Kirkcaldy, Brian A King, and John T Brooks. COVID-19 and postinfection immunity: Limited evidence, many remaining questions. *JAMA*, 2020.

[40] Andreas Kronbichler, Daniela Kresse, Sojung Yoon, Keum Hwa Lee, Maria Effenberger, and Jae Il Shin. Asymptomatic patients as a source of COVID-19 infections: A systematic review and meta-analysis. *International Journal of Infectious Diseases*, 2020.

[41] Lei Huang, Xiuwen Zhang, Xinyue Zhang, Zhijian Wei, Lingli Zhang, Jingjing Xu, Peipei Liang, Yuanhong Xu, Chengyuan Zhang, and Aman Xu. Rapid asymptomatic transmission of COVID-19 during the incubation period demonstrating strong infectivity in a cluster of youngsters aged 16-23 years outside Wuhan and characteristics of young patients with COVID-19: a prospective contact-tracing study. *Journal of Infection*, 2020.

[42] Enrico Lavezzo, Elisa Franchin, Constanze Ciavarella, Gina Cuomo-Dannenburg, Luisa Barzon, Claudia Del Vecchio, Lucia Rossi, Riccardo Manganelli, Arianna Loregian, Nicolò Navarin, et al. Suppression of COVID-19 outbreak in the municipality of Vo, Italy. *Nature*, 2020.

[43] Nguyen Van Vinh Chau, Vo Thanh Lam, Nguyen Thanh Dung, Lam Minh Yen, Ngo Ngoc Quang Minh, Le Manh Hung, Nghiem My Ngoc, Nguyen Tri Dung, Dinh Nguyen Huy Man, Lam Anh Nguyet, et al. The natural history and transmission potential of asymptomatic SARS-CoV-2 infection. *Clinical Infectious Diseases*, 2020.

[44] Robert Koch Institut. Epidemiologisches Bulletin 32/33 2020. `https://www.rki.de/DE/Content/Infekt/EpidBull/Archiv/2020/Ausgaben/32-33_20.pdf`, 2020. Accessed: 2020-08-27.

[45] Josh A Firth, Joel Hellewell, Petra Klepac, Stephen M Kissler, Adam J Kucharski, Lewis G Spurgin, CMMID COVID-19 working group, et al. Combining fine-scale social contact data with epidemic modelling reveals interactions between contact tracing, quarantine, testing and physical distancing for controlling COVID-19. *medRxiv*, 2020.

[46] Alberto Aleta, David Martin-Corral, Ana Pastore y Piontti, Marco Ajelli, Maria Litvinova, Matteo Chinazzi, Natalie E Dean, M Elizabeth Halloran, Ira M Longini Jr, Stefano Merler, et al. Modeling the impact of social distancing, testing, contact tracing and household quarantine on second-wave scenarios of the COVID-19 epidemic. *medRxiv*, 2020.

[47] Simone Sturniolo, William Waites, Tim Colbourn, David Manheim, and Jasmina Panovska-Griffiths. Testing, tracing and isolation in compartmental models. *medRxiv*, 2020.

[48] Sheng-Chia Chung, Sushila Marlow, Nicholas Tobias, Ivano Alogna, Alessio Alogna, and San-Lin You. A rapid systematic review and case study on test, contact tracing, testing, and isolation policies for COVID-19 prevention and control. *medRxiv*, 2020.

[49] Melissa Eddy. Welcome Back to Germany. Now Take Your Free Virus Test. *The New York Times*, August 2020.

[50] Xi He, Eric HY Lau, Peng Wu, Xilong Deng, Jian Wang, Xinxin Hao, Yiu Chung Lau, Jessica Y Wong, Yujuan Guan, Xinghua Tan, et al. Temporal dynamics in viral shedding and transmissibility of COVID-19. *Nature Medicine*, pages 1–4, 2020.

[51] Sadamori Kojaku, Laurent Hébert-Dufresne, and Yong-Yeol Ahn. The effectiveness of contact tracing in heterogeneous networks. *arXiv preprint arXiv:2005.02362*, 2020.

[52] Ioanna Smyrlaki, Martin Ekman, Martin Vondracek, Natali Papanicoloau, Antonio Lentini, Johan Aarum, Shaman Muradrasoli, Jan Albert, Björn Högberg, and Björn Reinius. Massive and rapid COVID-19 testing is feasible by extraction-free SARS-CoV-2 RT-qPCR. *medRxiv*, 2020.

[53] Jessica Watson, Penny F Whiting, and John E Brush. Interpreting a COVID-19 test result. *Bmj*, 369, 2020.

[54] Ralf L. Schlenger. PCR-Tests auf SARS-CoV-2: Ergebnisse richtig interpretieren. *Dtsch Arztebl International*, 117(24):A–1194–, 2020.

[55] Andrew N Cohen and Bruce Kessel. False positives in reverse transcription PCR testing for SARS-CoV-2. *medRxiv*, 2020.

[56] Giulia Cencetti, Gabriele Santin, Antonio Longa, Emanuele Pigani, Alain Barrat, Ciro Cattuto, Sune Lehmann, and Bruno Lepri. Using real-world contact networks to quantify the effectiveness of digital contact tracing and isolation strategies for COVID-19 pandemic. *medRxiv*, 2020.

[57] Matthias an der Heiden and Osamah Hamouda. Schätzung der aktuellen entwicklung der SARS-CoV-2-Epidemie in Deutschland – Nowcasting. *Epidemiologisches Bulletin*, 2020(17):10–15, 2020.

[58] Stephen A Lauer, Kyra H Grantz, Qifang Bi, Forrest K Jones, Qulu Zheng, Hannah R Meredith, Andrew S Azman, Nicholas G Reich, and Justin Lessler. The incubation period of coronavirus disease 2019 (COVID-19) from publicly reported confirmed cases: estimation and application. *Annals of internal medicine*, 2020.

[59] Lawrence F Shampine and Mark W Reichelt. The MATLAB ode suite. *SIAM journal on scientific computing*, 18(1):1–22, 1997.

[60] Yousef Alimohamadi, Maryam Taghdir, Mojtaba Sepandi, I Md Ady Wirawan, Pande Putu Januraga, Hyung-Ju Kim, Hyun-Seong Hwang, Yong-Hyuk Choi, Hye-Yeon Song, Ji-Seong Park, et al. Estimate of the basic reproduction number for COVID-19: A systematic review and meta-analysis. *J Prev Med Public Health*, 53(3):151–157, 2020.

[61] Ann Barber, John M Griffin, Miriam Casey, Aine Collins, Elizabeth A Lane, Quirine Ten Bosch, Mart De Jong, David Mc Evoy, Andrew W Byrne, Conor G McAloon, et al. The basic reproduction number of SARS-CoV-2: a scoping review of available evidence. *medRxiv*, 2020.

[62] Sebastián Contreras, Juan Pablo Biron-Lattes, H. Andrés Villavicencio, David Medina-Ortiz, Nyna Llanovarced-Kawles, and Álvaro Olivera-Nappa. Statistically-based methodology for revealing real contagion trends and correcting delay-induced errors in the assessment of COVID-19 pandemic. *Chaos, Solitons & Fractals*, 139:110087, 2020.
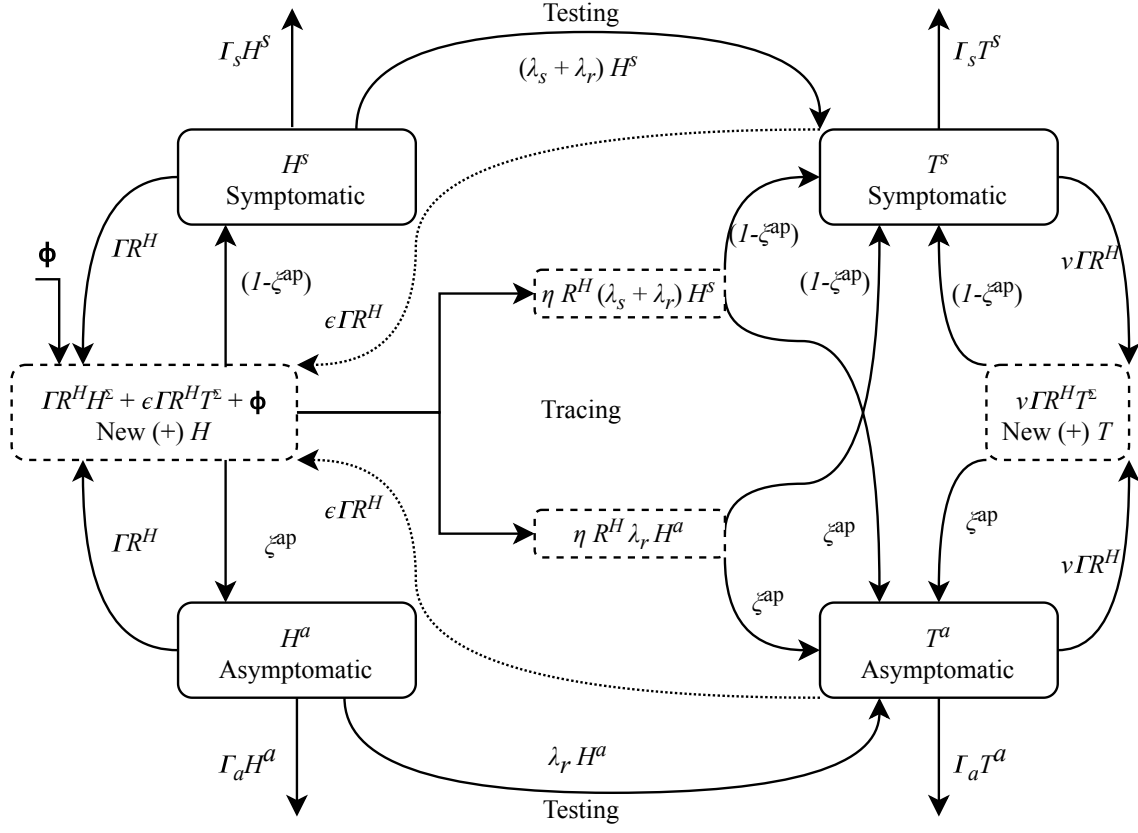
Figure S1: **Flowchart of the complete model.** This figure corresponds to Fig. 2 in the main manuscript.

[63] An Pan, Li Liu, Chaolong Wang, Huan Guo, Xingjie Hao, Qi Wang, Jiao Huang, Na He, Hongjie Yu, Xihong Lin, et al. Association of public health interventions with the epidemiology of the COVID-19 outbreak in Wuhan, China. *Jama*, 323(19):1915–1923, 2020.

[64] Feng Pan, Tianhe Ye, Peng Sun, Shan Gui, Bo Liang, Lingli Li, Dandan Zheng, Jiazheng Wang, Richard L Hesketh, Lian Yang, et al. Time course of lung changes on chest CT during recovery from 2019 novel coronavirus (COVID-19) pneumonia. *Radiology*, page 200370, 2020.

[65] Worldometers.info. Official numbers for the coronavirus outbreak worldwide. `https://www.worldometers.info/coronavirus/`, 20 May, 2020. Accessed: 2020-05-20.

[66] Yun Ling, Shui-Bao Xu, Yi-Xiao Lin, Di Tian, Zhao-Qin Zhu, Fa-Hui Dai, Fan Wu, Zhi-Gang Song, Wei Huang, Jun Chen, et al. Persistence and clearance of viral RNA in 2019 novel coronavirus disease rehabilitation patients. *Chinese medical journal*, 2020.

Supplementary Material

On the linear stability of the system

For analyzing the stability of the governing differential equations, namely, whether an outbreak could be controlled, we studied the linear stability of the system. The linearized system for equations (1)-(3) with limitless tracing capacity, is given by:

$$\frac{d}{dt}\begin{pmatrix} T \\ H \\ H^s \end{pmatrix} = \begin{pmatrix} \Gamma\left(\nu R_t^H - 1\right) & \lambda_r\left(\eta R_t^H + 1\right) & \lambda_s\left(1 + \eta R_t^H\right) \\ \Gamma\epsilon R_t^H & \Gamma\left(R_t^H - 1\right) - \lambda_r\left(1 + \eta R_t^H\right) & -\lambda_s\left(1 + \eta R_t^H\right) \\ \left(1-\xi^{\mathrm{ap}}\right)\Gamma\epsilon R_t^H & \left(1-\xi^{\mathrm{ap}}\right)\left(\Gamma R_t^H - \lambda_r\left(1 + \eta R_t^H\right)\right) & -\eta\left(1-\xi^{\mathrm{ap}}\right)R_t^H\lambda_s - \left(\lambda_s + \lambda_r + \Gamma\right) \end{pmatrix}\begin{pmatrix} T \\ H \\ H^s \end{pmatrix}$$
$$\text{(S1)}$$

By studying the eigenvalues of the associated matrix we can infer the stability of the solutions around the equilibrium. In particular, we define R_{crit}^H as the largest R_t^H such that the real part of $\mu_{\max}$, the largest eigenvalue of matrix A, is strictly negative.

Equilibrium equations

A system equilibrium is reached when time derivatives equals zero. That is by setting the left hand side in eqs. (1)-(3) equal to zero, e.g., $dT/dt = 0$. Regarding the SIR-like model presented here, an equilibrium with non-zero new cases can be attained for a positive constant influx Φ and certain combination of the parameters, depending on whether the health authority's tracing capacity is exceeded or not. For the case in which it is not exceeded, the equilibrium is stable as soon as $R_t^H < R_{\text{crit}}^H$ (R_{crit}^H is calculated in Table 1) and given by the following set of equations:

$$T_e = \frac{\Phi}{\Gamma\left(1 - \nu R_t^H\right)} \left[\left(\frac{\epsilon R_t^H}{\nu R_t^H - 1} + R_t^H \right) - \left(R_t^H - 1 \right) \frac{\eta R_t^H + \frac{1 + \Gamma/\lambda_s}{1 - \xi^{\text{ap}}}}{\eta R_t^H + 1} \right]^{-1} \tag{S2}$$

$$H_e = \frac{\Phi}{\Gamma\left(R_t^H - 1\right)} \left(\left[\left(\frac{\epsilon R_t^H}{\nu R_t^H - 1} + R_t^H \right) - \left(R_t^H - 1 \right) \frac{\eta R_t^H + \frac{1 + \Gamma/\lambda_s}{1 - \xi^{\text{ap}}}}{\eta R_t^H + 1} \right]^{-1} \left(1 + \frac{\epsilon R_t^H}{\nu R_t^H - 1} \right) - 1 \right) \tag{S3}$$

$$H_e^s = \frac{\Phi}{\lambda_s\left(1 + \eta R_t^H\right)} \left[\left(\frac{\epsilon R_t^H}{\nu R_t^H - 1} + R_t^H \right) - \left(R_t^H - 1 \right) \frac{\eta R_t^H + \frac{1 + \Gamma/\lambda_s}{1 - \xi^{\text{ap}}}}{\eta R_t^H + 1} \right]^{-1} \tag{S4}$$

Otherwise, when the tracing capacity is exceeded ($\eta \lambda_s R_t^H H_e^s > n_{\max}$), the equilibrium determined by:

$$T_e = \frac{-\left(\lambda_s H_e^s + n_{\max}\right)}{\Gamma\left(\nu R_t^H - 1\right)} \tag{S5}$$

$$H_e = \frac{\left(\lambda_s H_e^s + n_{\max}\right)}{\Gamma\left(R_t^H - 1\right)} \left[1 + \frac{\epsilon R_t^H}{\nu R_t^H - 1} - \frac{\Phi}{\Gamma\left(R_t^H - 1\right)} \right] \tag{S6}$$

$$H_e^s = \frac{n_{\max}\left(\frac{\epsilon R_t^H}{\nu R_t^H - 1} + 1 \right) - \Phi}{\frac{\left(R_t^H - 1\right)\left(\lambda_s + \Gamma\right)}{1 - \xi^{\text{ap}}} - R_t^H \lambda_s \left(1 + \frac{\epsilon}{\nu R_t^H - 1} \right)} \tag{S7}$$

It is important to note that an equilibrium can be reached even if the number of individuals entering the hidden pool is different from zero. This equilibrium exhibits a stable number of daily new cases.

Parameter uncertainty propagation

Table S1: Parameter uncertainty propagation

| Parameter	Meaning	Mean	95% CI	α	β	Dist.	Units
ξ^{ap}	Apparent Asymptomatic ratio	0.32	0.19–0.47	13.1	27.8	beta	—
λ_s	Symptom-driven test rate	0.10	0.05–0.16	10.7	96.3	beta	days^{-1}
ν	Isolation factor (traced)	0.10	0.03–0.22	3.5	31.5	beta	—
η	Tracing efficiency	0.66	0.59–0.73	117.9	60.7	beta	—
ϵ	Missed contacts (traced)	0.10	0.03–0.22	3.5	31.5	beta	—
$R_{\mathrm{crit}}^{H}\big|_{\eta=0.66}$	Critical reproduction number (hidden) (with $<\eta>= 0.66$)	1.90	1.42–2.70	—	—	—	—
$R_{\mathrm{crit}}^{H}\big|_{\eta=0}$	Critical reproduction number (hidden) (with $\eta = 0$)	1.42	1.23–1.69	—	—	—	—
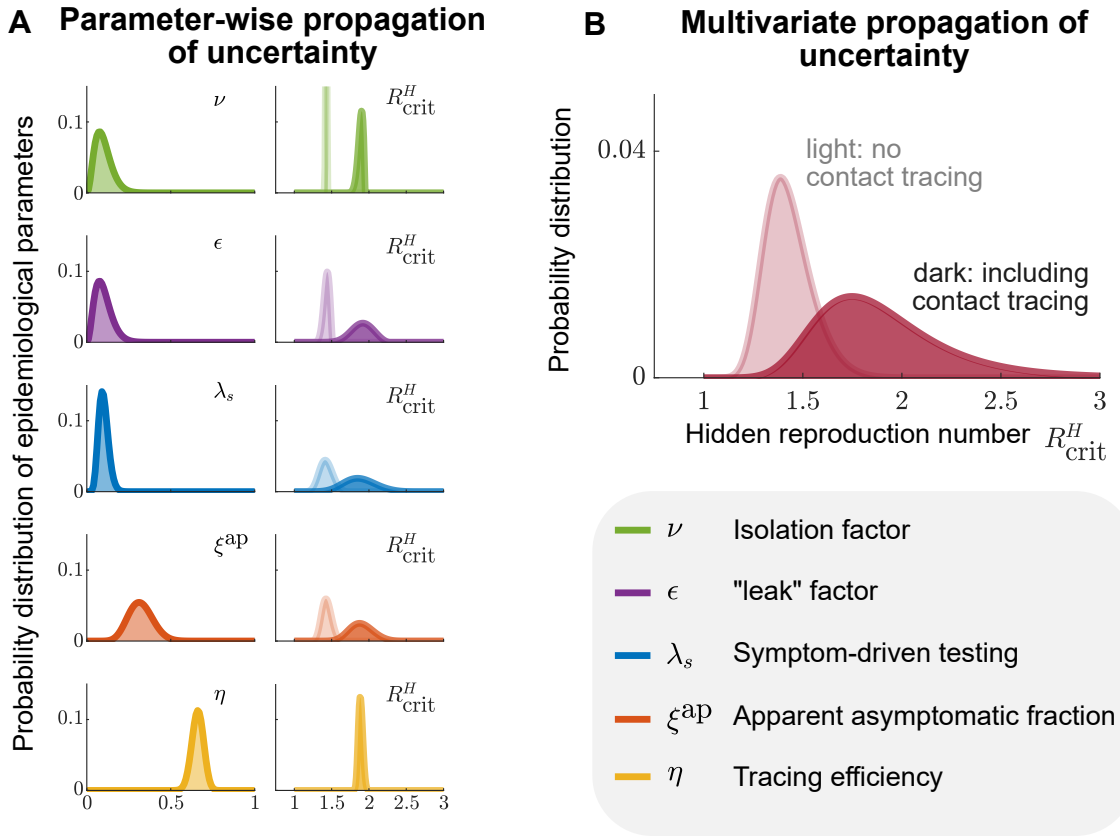
Figure S2: **Propagation of TTI-parameter uncertainties to the critical reproduction number.** As the different parameters involved in our model play different roles, the way their variability propagates to R_{crit}^{H} differs, even when their variability profiles look similar. **(A)** Univariate uncertainties of TTI parameters modelled by beta distributions centered on their default value (left column), and the resulting distribution of critical reproduction numbers (right column). Results are shown for the R_{crit}^{H} assuming testing only (light colors) or testing and tracing (dark colors). **(B)** Distribution of critical reproduction numbers arising from multivariate uncertainty propagation given by the joint of the distributions shown in (A) for testing only, or testing and tracing. Results show averages of 100 000 realizations.